ESTCP

FINAL REPORT

Integrated Microgrid Control Platform

Gabor Karsai
Vanderbilt University

Srdjan Lukic
North Carolina State University

March 2024

ESTCP Project EW20-5139

REPORT DOCUMENTATION PAGE

Form Approved
OMB No. 0704-0188

1. REPORT DATE *(DD-MM-YYYY)*	**2. REPORT TYPE**	**3. DATES COVERED** *(From - To)*
1-3-2024	ESTCP Final Report	7/31/2020 - 7/31/2024

4. TITLE AND SUBTITLE

Integrated Microgrid Control Platform (IMCP)

5a. CONTRACT NUMBER
W912HQ20C0040

5b. GRANT NUMBER

5c. PROGRAM ELEMENT NUMBER

6. AUTHOR(S)

Gabor Karsai and Srdjan Lukic

5d. PROJECT NUMBER
EW20-5139

5e. TASK NUMBER

5f. WORK UNIT NUMBER

7. PERFORMING ORGANIZATION NAME(S) AND ADDRESS(ES)

Vanderbilt University
1025 16th Avenue South,
Nashville, TN 37212

North Carolina State University,
1791 Varsity Drive, St100,
Raleigh, NC 27606

8. PERFORMING ORGANIZATION REPORT NUMBER

EW20-5139

9. SPONSORING / MONITORING AGENCY NAME(S) AND ADDRESS(ES)

Office of the Deputy Assistant Secretary of Defense (Energy Resilience & Optimization)
3500 Defense Pentagon, RM 5C646
Washington, DC 20301-3500

10. SPONSOR/MONITOR'S ACRONYM(S)
ESTCP

11. SPONSOR/MONITOR'S REPORT NUMBER(S)
EW20-5139

12. DISTRIBUTION / AVAILABILITY STATEMENT

DISTRIBUTION STATEMENT A: This document has been cleared for public release

13. SUPPLEMENTARY NOTES

14. ABSTRACT

Microgrids are increasingly being used as energy systems for military installations and forward deployed units. Microgrids are small-scale energy networks, and they typically include several alternative, distributed energy resources (DER) whose power delivery needs to be coordinated at different time scales (milliseconds, seconds, and hours). The main technical objective of the project was to demonstrate how foundational technology for microgrid control, can be applied in a field environment, on a realistic microgrid. The specific goals of the project were: (1) demonstrate advanced, distributed microgrid control algorithms that solve the dynamic, real-time reconfiguration and optimal dispatch problem of networked microgrids, (2) construct a concrete and functional demonstration based on a distributed software platform, and demonstrate it, as a reference implementation for future installations.

15. SUBJECT TERMS

Microgrid control systems, microgrids, Installation Resilience, Energy Resilience, adaptive control, interoperable

16. SECURITY CLASSIFICATION OF:			**17. LIMITATION OF ABSTRACT**	**18. NUMBER OF PAGES**	**19a. NAME OF RESPONSIBLE PERSON**
a. REPORT	**b. ABSTRACT**	**c. THIS PAGE**			Gabor Karsai
Unclassified	Unclassified	Unclassified	Unclassified	74	**19b. TELEPHONE NUMBER** *(include area code)* 615 343 7471

ESTCP FINAL REPORT

Project: EW20-5139

TABLE OF CONTENTS

Page

TABLE OF CONTENTS (Continued)

Page

LIST OF FIGURES

Page

LIST OF TABLES

Page

ACRONYMS AND ABBREVIATIONS

ARPA-E	Advanced Research Projects Agency - Energy
BES	Battery Energy System
CHP	Combined Heat and Power
DDC	DER Device I/O Component
DER	Distributed Energy Resource
DG	Distributed Generator
DIOC	Device I/O Component
DOS	Denial-Of-Service
DSP	Digital Signal Processing
ESTCP	Environmental Security Technology Certification Program
FSM	Finite-State Machine
GUI	Graphical User Interface
HIL	Hardware-In-the-Loop
IEEE	Institute of Electrical and Electronics Engineers
IMCP	Integrated Microgrid Control Platform
kVA	KiloVolt-Ampere
LAN	Local Area Network
MAC	Mandatory Access Control
MCC	Microgrid Computational Component
MG	Microgrid
MQTT	MQ Telemetry Transport
MVA	MegaVolt-Ampere
PMU	Phase Measurement Unit
POI	Point of Interconnect
PTP	Precision Time Protocol
PV	Photovoltaic Cell
PWM	Pulse Width Modulation
RCC	Relay Control Component
RIAPS	Resilient Information Architecture Platform for Smart Grid
RoCoF	Rate of Change of Frequency

SEL	Schweitzer Engineering Laboratories
SMC	State Machine Component
UPS	Uninterruptible Power Supply

ACKNOWLEDGEMENTS

This material is based upon work supported by the United States Army Corps of Engineers under Contract No. W912HQ20C0040 and the Department of Defense Environmental Security Technology Certification Program (ESTCP). Any opinions, findings and conclusions or recommendations expressed in this material are those of the author(s) and do not necessarily reflect the views of the United States Army Corps of Engineers or the DoD ESTCP.

ABSTRACT

INTRODUCTION AND OBJECTIVES. Microgrids are increasingly being used as energy systems for military installations and forward deployed units. Microgrids are small-scale energy networks, and they typically include several alternative, distributed energy resources (DER) whose power delivery needs to be coordinated at different time scales (milliseconds, seconds, and hours). The main technical objective of the project was to demonstrate how foundational technology for microgrid control, can be applied in a field environment, on a realistic microgrid. The specific goals of the project were: (1) demonstrate advanced, distributed microgrid control algorithms that solve the dynamic, real-time reconfiguration and optimal dispatch problem of networked microgrids, (2) construct a concrete and functional demonstration based on a distributed software platform, and demonstrate it, as a reference implementation for future installations.

TECHNOLOGY DESCRIPTION. The technology developed is a concrete implementation of advanced microgrid control algorithms that implement various transition and power management functions. Specifically, the algorithms implement control and management functions for: (1) power dispatch from microgrid DERs proportionally to their ratings, (2) grid support by microgrid DERs with frequency/Watt mode, (3) power factor control for grid support, (4) dispatch DER power to compensate for the loss of bus in grid-connected mode, (5) managing planned islanding transition, (6) managing unplanned (abrupt) islanding, (7) connecting two adjacent microgrids, (8) dispatch DER power to compensate for the loss of bus in islanded mode, (9) resynchronization and reconnection to main grid. The algorithms are implemented on a fully distributed, resilient computing platform.

PERFORMANCE AND COST ASSESSMENT. The project team developed, implemented, and validated a complete, distributed microgrid controller software package. The simulation-based evaluation has shown that the approach (1) enabled the formation of a network of microgrids with dynamic boundaries through platform group formation features, (2) supported the low-cost incremental expansion of networked distributed energy resources and critical loads through the platform's component plug-and-play architecture and reusable interfaces, (3) delivered inherent system resilience due to the distributed peer-to-peer control with no single point of failure and inherent cyber-security features, and (4) simplified the microgrid controller design process by reusing control algorithms and component interfaces through an open source code base of solutions.

IMPLEMENTATION ISSUES. The development project has not encountered any implementation issues. For fielding the results of the project, i.e., the control algorithm implementations state-of-the-art embedded, industrial-grade computing devices are needed, that have (1) local area network interfaces with support for IEEE 1588 - Precision Time Protocol (PTP), and (2) interfaces to local DER-s (e.g. Modbus of serial ports). The developed software code base: the microgrid controller and the software platform is open source, and as such can be used by developers of microgrids.

PUBLICATIONS. Hao Tu, Hui Yu, Yuhua Du, Scott Eisele, Xiaonan Lu, Gabor Karsai and Srdjan Lukic, "An IoT-based Framework for Distributed Generic Microgrid Controllers" Accepted for publication in *IEEE Transactions on Control Systems Technology.* The article summarizes the main results of the project.

EXECUTIVE SUMMARY

INTRODUCTION

Microgrids are increasingly being used as energy systems for military installations and forward deployed units. Microgrids are small-scale energy network, and they typically include several alternative, distributed energy resources (DER), like photovoltaic cells (PV), battery energy systems (BES), and diesel generators ('gensets') as energy sources, but they are also connected to the main utility grid, if needed. Energy is either supplied by the local DERs, or by the utility grid, but the microgrid could also supply power to the main grid.

Integration of heterogeneous generation sources and legacy devices into a DoD microgrid poses several hardware and software challenges: lack of advanced control algorithms, engineering processes for integrating various generation technologies, and the inherent complexities of system configuration and integration. Forming networked microgrids out of heterogeneous power sources adds more complexity due to the varying dynamics of the resources, potentially different communication protocols for each resource, and the required redesign of the protection systems. Further, the management of legacy loads presents another layer of complexity. A significant challenge here is to manage and control networks of microgrids, changing the system topology 'on the fly', i.e., while the system is operational.

A DoD Microgrid Control System is a mission- and safety-critical Industrial Control System (ICS), operating in a national security environment. But it is also a distributed system, implemented using computing and networking technologies that are potentially exposed to cyber threats. Hence, effort needs to be devoted to cyber-security to protect against various forms of cyber-attacks.

The IMCP project was designed and executed to address these issues. In subsequent sections summarize the objectives of the project and the technology developed, assess the performance and estimated costs, and discuss implementation issues. The summary concludes with outlining implications for future research and benefits for DoD.

OBJECTIVES

The objective of the research was to demonstrate advanced technology for microgrid integration and control, based on distributed computing techniques, advanced software engineering methods, cyber-security protections, and state-of-the-art control algorithms that provides a scalable and reusable solution, yielding a highly configurable Integrated Microgrid Control Platform (IMCP). This activity is directly related to the DoD Statement of Need for advanced, affordable, and resilient energy systems for military installations.

Here, the concept 'distributed' denotes an architecture where monitoring and control functions are implemented in a network of embedded computing nodes that are attached to key monitoring and control devices in a power network and communicate via a data network, collaborating in a peer-to-peer fashion. The solution developed by the project addresses the heterogeneity problem by encapsulating the specific details of protocols into reusable 'device components' with common interfaces, and the dynamic grid management and reconfiguration problem with advanced distributed algorithms that form the foundation for a decentralized and expandable microgrid controller.

The long-term vision of the project is that the distributed, open platform-based approach will not only enable technological advances, like intelligent energy management and networked microgrids, but will also reduce the engineering costs. Distributed systems also facilitate enhanced resilience through redundancy and provide opportunities for enhanced cyber protections. Arguably, distributed architectures could be made more resilient than centralized controllers, where the sole controller itself is a single point of failure.

However, these claims had to be validated in a HIL environment before fielding such systems. The goal of the project was to confirm these claims and to show how a resilient distributed microgrid control system can be built in a modular fashion, from pre-designed computational components, including advanced control algorithms and device protocol interfaces. This validation was performed through executing a suite of test scenarios in a high-fidelity, simulation-based Hardware-in-the-Loop environment that showed the level of maturity of the technology and its readiness for use in the field.

TECHNOLOGY DESCRIPTION

IMCP includes two technologies: (1) RIAPS, a software platform, and (2) a microgrid control and integration technology based on advanced, distributed, and resilient control algorithms, running on RIAPS. RIAPS has been supported by an earlier ARPA-E project, and it has been improved for the purposes of the project. The ESTCP program has supported (1) the implementation of the IMCP control algorithms and (2) the extensions to RIAPS to support device connectivity for the microgrid controller.

Resilient Information Architecture Platform (RIAPS)

RIAPS is a software platform: an 'operating system' for Smart Grid software, not unlike Android for smartphones that supports the construction and operation of distributed applications ('apps') that run on a network of field computing devices. It is based on a message-oriented software component model, where the applications are constructed from a network of interacting components (similar to 'agents', but more tuned for real-time performance) that exchange messages, but also communicate with local power system devices (e.g., PMUs, inverters, breakers, relays, etc.). RIAPS runs on small, inexpensive, embedded computing devices, and provides several services for messaging, dynamic application composition, resource management, distributed coordination among dispersed components, and fault tolerance. It also provides a foundation for strong cyber security, including encryption and Mandatory Access Control (MAC) for applications. RIAPS has a software development kit, including tools for application deployment and management, and is available under an open-source license. Figure 1 shows the software platform's architecture.

APS consists of two sets of software modules: (1) the component framework that includes support libraries to build distributed apps, and (2) the platform managers that includes service programs that assist with the remote installation, operation, security, and management of the apps.

RIAPS is a software layer above an underlying operating system (Real-time enabled Linux), and can support a variety of applications that implement various functions, like power management, secondary level microgrid control, etc. What RIAPS offers to developers is a set of services that help with building resilient, secure distributed applications. Each computing host ('RIAPS node') in a RIAPS network runs a copy of the platform, as shown on Figure 1.

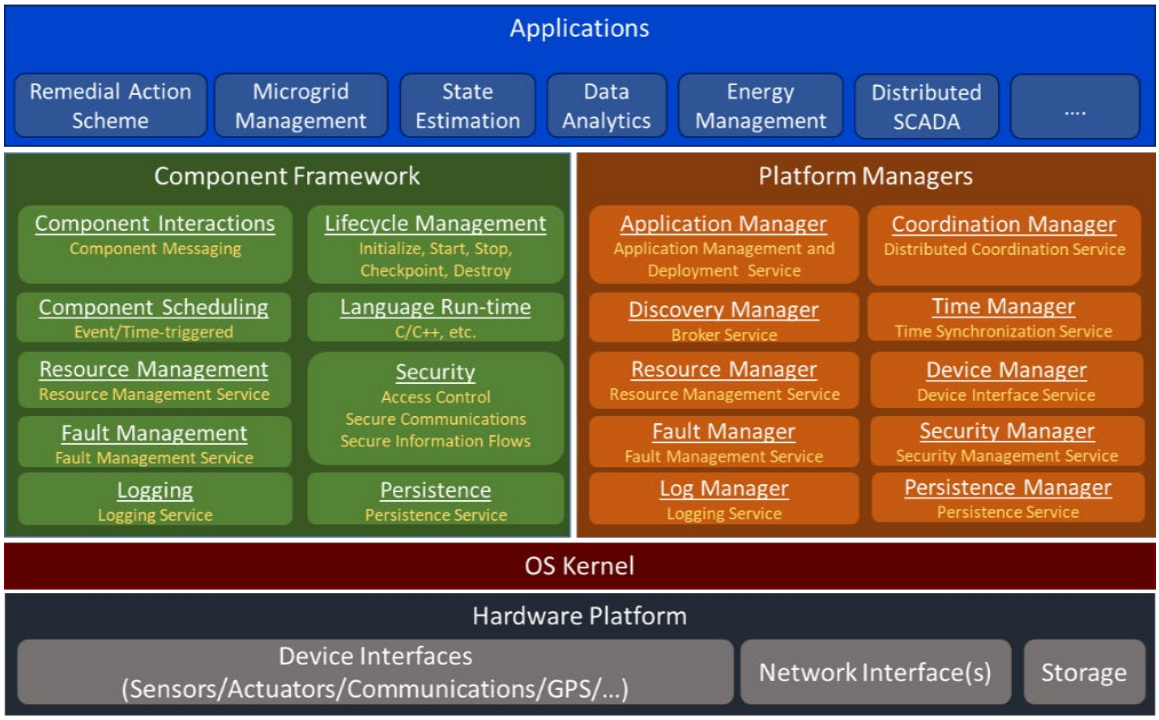

Figure 1. RIAPS Architecture

The functions of distributed applications arise from the interactions among computing nodes. Interactions are implemented as message exchanges, through which the application components share data and salient events. Each node is responsible for its own control actions, but it works with the other nodes to achieve overall control objectives.

There are several features in RIAPS to facilitate this paradigm, including support for fault detection, isolation, and recovery, high-precision clock synchronization across the network, real-time scheduling, and encrypted and authenticated communications.

Distributed Microgrid Controller

The microgrid controller algorithm manages (1) islanded operation, including energy management functions and emergency dispatch order functions based on the energy management goals defined by the use case; (2) grid connected operation, including demand response, and methodologies to reduce demand charges, based on the information provided about the site; (3) transition functions that ensure planned and unplanned seamless transition from grid connected to islanded operation and back to grid connected mode and (4) black start functionality. Thus, the microgrid controller design provides for all the functional requirements that ensure a technically sound operation of the microgrid, per the IEEE 2030.7 standard. The standard defines the microgrid operating modes and transitions among them, as shown on Figure 2.

Conventional microgrid controllers implement these functions using a centralized architecture, where each DG can be individually monitored and controlled, but the actual control function is implemented in a single, central controlling computer. This solution leads to potential problems with fault-tolerance: the centralized controller is a single point of failure. Furthermore, the network round-trip time between the DG and the centralized controller can be unacceptable.

Another disadvantage of a centralized controller is the rigidity of the boundaries between microgrids, where combining microgrids with separate MG controllers becomes a control challenge as does changing the boundaries of the existing microgrid as the system gets reconfigured. In a distributed paradigm changing microgrid boundaries, adding resources to a microgrid controller and commanding microgrids is seamlessly managed by a membership function that defines the communication links, without the necessity to change the underlying management algorithms.

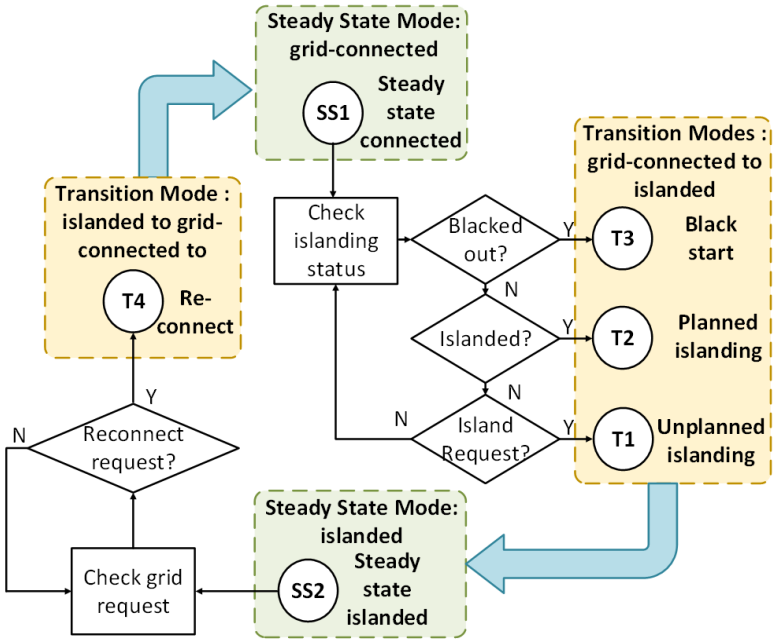

Figure 2. MG Operation Modes per IEEE Std. 2030.7

To address these shortcomings, IMCP implements these functions in a fully distributed architectures as illustrated on Figure 3. In this architecture, each DG has its own local controller, which exchanges data with other controllers connected to the same network. Each local controller is capable of operating independently, although with degraded performance, even if connectivity to the network is lost. This provides resilience for the overall system. If the local controller is connected to its peers, coordination is possible, and the system is operating with high performance. The distributed microgrid controller IMCP has been implemented as a RIAPS 'application'.

The microgrid controller application coordinates a set of low-capacity distributed generators (DG) to achieve a system-level goal. As a power system, this is different from many state-of-the art microgrid implementations where one large energy storage unit has sufficient capacity to smooth out the system dynamics and acts as the "grid forming" unit in islanded mode. In islanded operating mode and for microgrid synchronization to the main grid, the DG assets coordinate to proportionally share the real and reactive power system load while restoring the microgrid voltage and frequency and eliminating the amplitude and phase differences between the voltages on either side of the relay at the point of interconnection. The approach uses pinning-based consensus algorithms to coordinate among the DG assets. Other applications use a similar approach to coordinate assets in neighboring microgrids to achieve seamless connection and islanded operation of adjacent microgrids and thus supply critical loads when facing system contingencies or fault conditions.

Note that these algorithms can manage networked microgrid as well. These distributed applications make use of the consensus-based algorithms implemented on the RIAPS platform, the platform group formation and time synchronization functionalities.

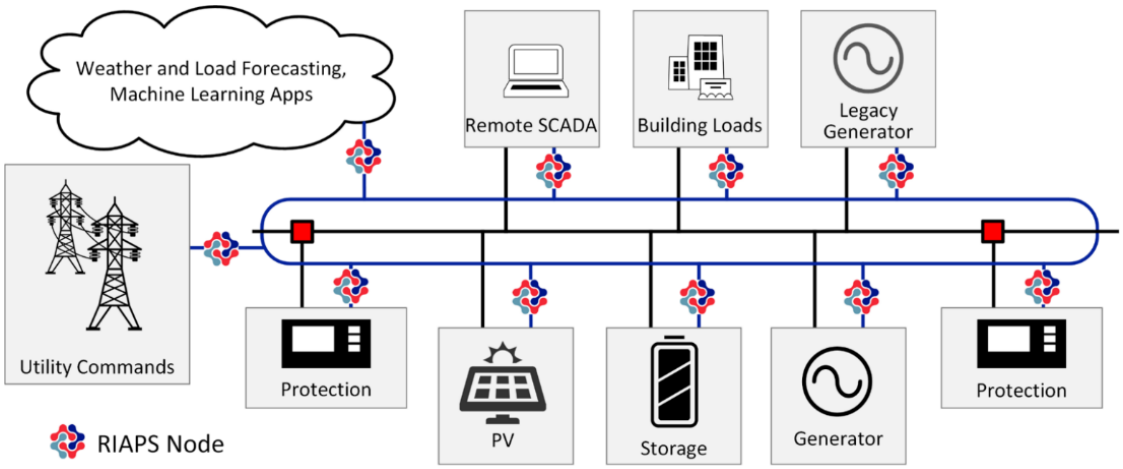

Figure 3. Distributed Microgrid Control Application: IMCP Built with RIAPS

The IMCP was designed to be a highly configurable software system. Each device interface that connects the controller software to actual physical inverters, relays, gensets, etc., is customizable to specific device addresses accessible via the Modbus protocol. The controller algorithms coefficients, i.e., the controller gains are also customizable for specific functions. Furthermore, the IMCP has been extended with a simple graphical user interface that allows the visualization of the one-line diagram of the microgrid's circuits, and these user interfaces can also be customized to specific data points, sensed or controlled, available in the actual instance of the IMCP application, for a given microgrid.

The benefit of the approach is in the reusability of the algorithms and the interfaces across many DoD installations and microgrid use cases though the development of highly configurable and reusable software components. We envision that controllers for new microgrid configurations can be inexpensively constructed by composing ('wiring') and parameterizing existing software components. Our approach builds on an open-source platform that allows for easy integration of state of the art and legacy equipment into a microgrid management system. Different from other commercial offerings, the developed solution is (1) fully open source - allowing for applications, component interfaces, energy management and power management algorithms to be used across any number of installations and use cases; (2) the approach is distributed - allowing for simple system scaling, and reconfiguration, as the microgrid grows, or as the boundaries of the microgrid and its critical loads move. While existing state of the art solutions are designed to be closed to the user and are typically designed to be centralized. The life cycle cost advantage comes from the reusability of the interfaces and algorithms.

Implementation and Testing

The IMCP has been implemented and tested for a modified version of the Banshee microgrid system. The implementation software architecture is shown on. The modified one-line diagram of the microgrid is shown on **Figure 5**.

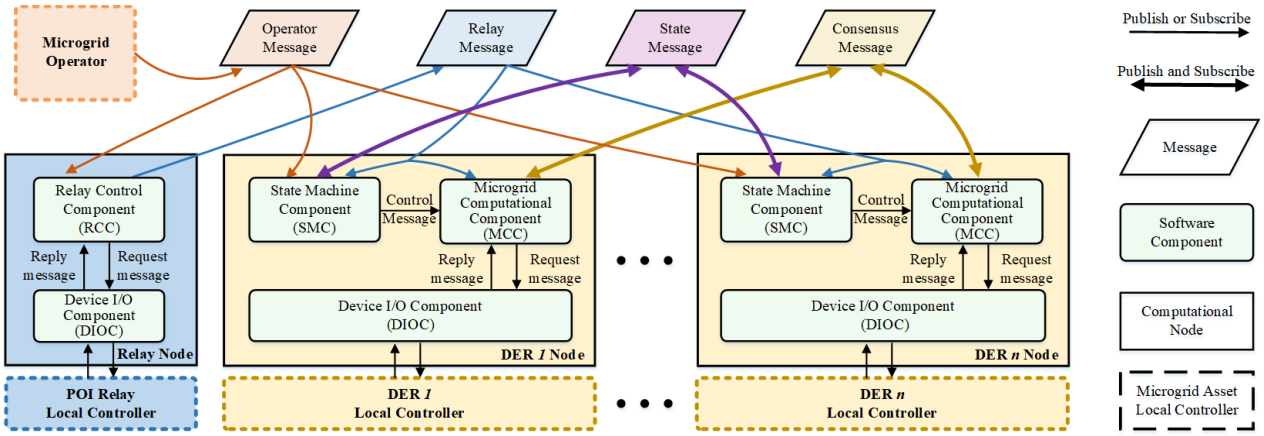

Figure 4. Implementation Architecture

The testing involved hardware-in-the-loop (HIL) testing against a high-fidelity real-time simulation model of the microgrid that was running on an OPAL-RT simulator. The tests included microgrid functionality tests and cyber-security tests, summarized on Table 1.

The microgrid controller software was running on a network of small, embedded computing devices: Beaglebone Black boards, that were connected to an Ethernet-based Local Area Network (LAN) on one side and to the real-time simulator on the other side. While both connections were done via the Ethernet connectors and via the TCP/IP protocol, the connection to the simulator was using the Modbus/TCP-IP protocol; an industry standard for communicating with power system devices.

Table 1. Summary of Tests

Mode	Tests	Result – Demonstrated IMCP capability
Grid-connected	HIL1: Power Dispatch at POI	Dispatching real and reactive power from the microgrid DER-s proportionally to their ratings
	HIL2: Grid support at POI	Frequency/Watt mode dynamic reactive power support
	HIL 3: Power Factor Control at POI	Power factor control to support the main grid
	HIL 4: Loss of bus (load pickup)	Dispatching power to compensate for loss of bus
Islanding	HIL.5: Disconnect command (Planned Islanding)	Maintain control of the microgrid in case of planned islanding
	HIL.6: Unplanned disconnect (Unplanned Island)	Maintain control of the microgrid in case of unplanned, abrupt islanding
Islanded	HIL.7: Connect two adjacent microgrids (Reconfiguration)	Maintaining control while feeders are connected/disconnected
	HIL.8: Loss of bus (Load pickup)	Dispatching power to compensate for loss of bus
Islanded to grid-connected	HIL.9: Reconnect to the main grid	Facilitating seamless transition to grid-connected mode by controlling voltage/frequency/phase angel to achieve zero power transfer at POI.
Cybersecurity	CS.1: Confidentiality	Strong encryption of all network messages of application.
	CS.2: Integrity	Modified network messages are automatically rejected.
	CS.3: Authenticity	Network packets of invalid source are rejected.
	CS.4: Availability	Controller remains functional under network overload (DOS) conditions.

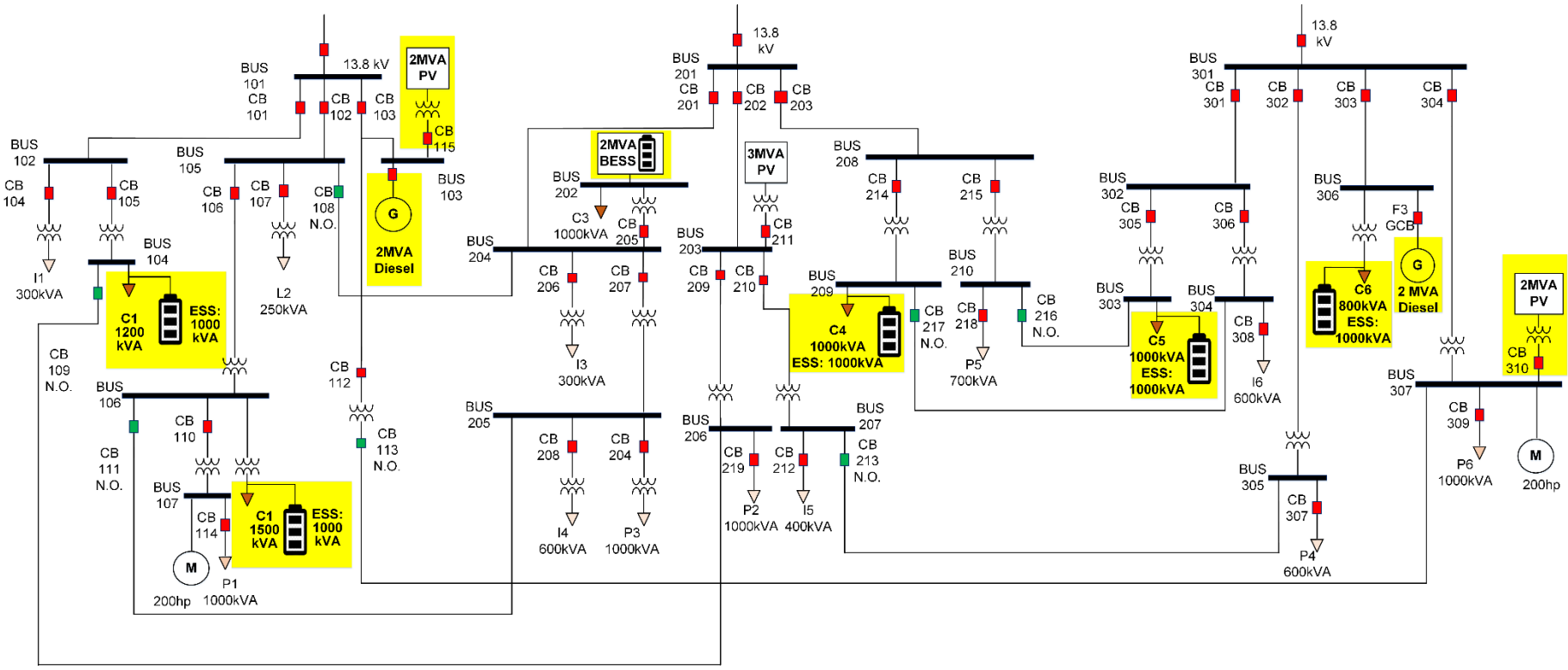

Figure 5. Test example: Modified Banshee Microgrid

The testing results show that the IMCP meets the functional and performance requirements. As outlined in Table 1, the proposed and adopted test plan considers various scenarios of system operation in grid connected and islanded mode and considers various transition scenarios from the two steady-state operating modes. The team implemented this test procedure on the testbed described earlier and found that the developed MG controller successfully met the performance metrics defined in the test plan.

The cyber-security tests have been executed by monitoring the network packets (CS.1), monitoring the behavior of the application (CS.2 and C S.3), and observing the performance of the controller under adversary conditions (CS.4). The tests have verified that only encrypted messages were sent through the network (CS.1), that tampered and invalid messages were rejected before reaching the application code, and that the controller remained functional even if node became isolated due to a Denial-Of-Service (DOS) attack. As expected, the controller remained functional, although with lower performance, due to the lost messages. Once the attack ceased, the controller recovered.

PERFORMANCE ASSESSMENT

The project has implemented the test procedure on a HIL setup that allows for the monitoring of the system voltage and frequency throughout the test. The relevant voltage and frequency measurement were taken at all buses of the microgrids and the results show that the system met the performance requirements throughout the test. The key metric of interest was that the voltage and frequency of the system remained within the allowable IEEE 1547 range in all conditions.

Grid-connected mode test scenarios

Functionality tested	Criteria met
HIL.1: PQ dispatch	Value within 5% of rating within 30 seconds (IEEE 1547-2018 clauses 4.4)
HIL.2: Frequency Watt Mode; Dynamic Reactive Power Support	Value within 5% within 30 seconds (IEEE 1547-2018 clauses 4.4)
HIL.3: PF command	Value within 5% of rating within 30 seconds (IEEE 1547-2018 clauses 4.4)
HIL.4: Loss of bus (Load Pickup)	Downstream loads picked up within 30 seconds.

Islanded mode and grid to island transition test scenarios

Functionality tested	Criteria met
HIL.5: Disconnect command (Planned Island)	Seamless transition from grid connected to islanded mode at prescribed time. V,f within allowable bands throughout.
HIL.6: Unplanned disconnect (Planned Island)	Seamless transition from grid connected to islanded mode at prescribed time. V,f within allowable bands throughout.
HIL.7: Connect two adjacent microgrids (reconfiguration)	Seamless connection of two islanded MG. V,f within allowable bands throughout.
HIL.8: Loss of bus (Load pickup)	Downstream loads picked up within 30 seconds.

Island to grid transition test scenario

Functionality tested	Criteria met
HIL.9: Reconnect to the main grid	Seamless transition from islanded to grid connected mode within prescribed time. V,f within allowable bands throughout.

Cyber-security test scenarios

Concern tested	Attacker action	Criteria met
CS.1: Confidentiality	Snoop on network packets	Attacker is unable to decode content
CS.2: Integrity	Modify and retransmit modified network packets	Modified packet is rejected by recipient
CS.3: Authenticity	Spoof network packets	Modified packet is rejected by recipient
CS.4: Availability	Flood network with packets	Controller app detects the problem and acts accordingly

COST ASSESSMENT

The developed IMCP implementation is a fully functional prototype, and it is available under an open source license. Open source license applies to the entire software stack: the operating system (Linux), several software packages (e.g. Python, and others), the RIAPS platform, and the IMCP itself. RIAPS and IMCP uses the Apache 2.0 license. All these licenses permit the use of the software as is, as well as its modification and distribution. To summarize, the software itself, in its current form, is available for use, with no cost.

However, if the software is used for another microgrid than the Banshee example (with Modbus/ TCP/IP interfaces) it needs to be configured, possibly customized and extended for a new microgrid.

The costs of using IMCP in a microgrid therefore includes: customizing it to the specific microgrid, developing and configuring new software interfaces (if needed), and testing, installing, and maintaining it.

The software needs a computing and network hardware. The actual controller software runs on small, networked embedded computers, while an additional computer is used to load and install the controller on the networked machines. For field installations, it is recommended to use industrial grade embedded computers, as well as industrial quality LAN.

IMPLEMENTATION ISSUES

The development project has not encountered any significant implementation issues. The implementation and its testing were performed in a laboratory environment, using simulated power systems. The simulator was a high-performance, high-fidelity, real-time simulator (OPAL-RT), that also implemented the real-time hardware/software interfaces (specifically: the Modbus protocol) that is expected in a field environment. The IMCP software was running on a network of Beaglebone Black devices: small form factor, embedded computing devices, connected to an isolated LAN in the lab.

However, for fielding the results of the project, i.e., the control algorithm implementations state-of-the-art embedded, industrial-grade computing devices are needed, that have (1) local area network interfaces with support for IEEE 1588 - Precision Time Protocol (PTP), and (2) interfaces to local DER-s (e.g. Modbus of serial ports). The industrial embedded computers need to be housed in field-grade enclosures, must have uninterruptible power supplies (UPS), and need to connect to a local area network. The interfaces to the power devices need to be designed according to the requirements of the field environment. The developed software code base: the microgrid controller and the software platform is open source, and as such can be used by developers of microgrids. However, it is necessary to customize it to a specific microgrid configuration and power system device.

1.0 INTRODUCTION

Microgrids are increasingly being used as energy systems for military installations and forward deployed units. Microgrids are small-scale energy networks, and they typically include several alternative, distributed energy resources (DER), like photovoltaic cells (PV), battery energy systems (BES), and diesel generators ('gensets') as energy sources, but they are also connected to the main utility grid, if needed. Energy is either supplied by the local DERs, or by the utility grid, but the microgrid could also supply power to the main grid.

1.1 BACKGROUND

The memorandum from the Office of Undersecretary of Defense from May 2021 titled "Metrics and Standards for Energy Resilience at Military Installations" [1] clearly states:

Planning and programming for energy resilience and energy security shall … promote the installation of cyber-resilient microgrids to ensure the energy security and energy resilience of critical missions

as well as

Energy resilience solutions can and should include integrated, distributed, on-site sources, energy storage, generation capable of accepting multiple fuel sources, quick connects for portable generation, and microgrids and centralized generation; diversified or alternative fuel supplies; relocating missions to alternative locations; and upgrading, replacing, and maintaining current energy systems, infrastructure, and equipment on DoD installations.

Microgrids clearly satisfy the stated requirements for 'energy resilience solutions,' as stated above. The work on this project was focusing on the control software needed for implementing microgrids. Based on informal discussions with industry, today's practice is to use one-off microgrid controllers, typically provided by large suppliers (e.g., SEL) that are centralized, inflexible, and lock-in the customer. The project aimed at changing this paradigm by developing and demonstrating a distributed microgrid controller.

The project was based on prior research, funded by DOE ARPA-E that was done earlier by the members of the team on microgrid controls. The prior research provided the software platform RIAPS, as described below. The work on this project has extended RIAPS with new capabilities and designed, implemented, and tested the IMCP microgrid controller algorithms.

The project has demonstrated a functional, fully distributed microgrid controller that can support control functions specified in the IEEE standards, and the performance of the controller satisfies the requirements. The controller software is generic, and can customized the specific microgrid installations. Because it is available under an open source license, it can reduce the software engineering costs whenever a new microgrid is needed. Furthermore, it offers a novel capability: it can control networked microgrids. Such microgrids offer a very flexible and robust architecture, that is scalable to the actual needs and can mitigate faults by reconfiguring the topology.

1.2 OBJECTIVE OF THE DEMONSTRATION

The *objective* of the research was to demonstrate advanced technology for microgrid integration and control, based on distributed computing techniques, advanced software engineering methods, cyber-security protections, and state-of-the-art control algorithms that provides a scalable and reusable solution, yielding a highly configurable Integrated Microgrid Control Platform (IMCP).

The activities of this project are directly related to the DoD Statement of Need for advanced, affordable, and resilient energy systems for military installations. A distributed microgrid controller that is performant, extensible, tolerant to faults in computing and communication hardware and software, and can manage networked microgrids is clearly addressing the need for software that can operate advanced, affordable, and resilient energy systems and military installations.

In the context of the project, the concept 'distributed' denotes an architecture where monitoring and control functions are implemented in a network of embedded computing nodes that are attached to key monitoring and control devices in a power network and communicate via a data network, collaborating in a peer-to-peer fashion. The solution developed by the project addresses the heterogeneity problem by encapsulating the specific details of protocols into reusable 'device components' with common interfaces, and the dynamic grid management and reconfiguration problem with advanced distributed algorithms that form the foundation for a decentralized and expandable microgrid controller

The specific *goal* of the demonstration was to show that the distributed microgrid controller is capable of performing control functions on a realistic microgrid and its performance complies with the IEEE standards requirements.

The long-term vision of the project is that the distributed, open platform-based approach will not only enable technological advances, like intelligent energy management and networked microgrids, but will also reduce the engineering costs. Distributed systems also facilitate enhanced resilience through redundancy and provide opportunities for enhanced cyber protections. Arguably, distributed architectures could be made more resilient than centralized controllers, where the sole controller itself is a single point of failure.

However, these claims had to be validated in a HIL environment before fielding such systems. The goal of the project was to confirm these claims and to show how a resilient distributed microgrid control system can be built in a modular fashion, from pre-designed computational components, including advanced control algorithms and device protocol interfaces. This validation was performed through executing a suite of test scenarios in a high-fidelity, simulation-based Hardware-in-the-Loop environment that showed the level of maturity of the technology and its readiness for use in the field.

1.3 REGULATORY DRIVERS

According to the knowledge of the authors of this report currently there are no federal, state, and local regulations that have resulted in a need for a new technology. The DoD directive [1] quoted in the Background section is the source that motivates the need for a new technology that can solve the microgrid control problem in a practical and robust manner.

2.0 TECHNOLOGY DESCRIPTION

2.1 TECHNOLOGY DESCRIPTION

IMCP includes two technologies: (1) RIAPS, a software platform, and (2) a microgrid control and integration technology based on advanced, distributed, and resilient control algorithms, running on RIAPS. RIAPS has been supported by an earlier ARPA-E project, and it has been improved for the purposes of the project. The ESTCP program has supported the implementation of the IMCP control algorithms and the extensions to RIAPS to support device connectivity for the microgrid controller.

2.1.1 Resilient Information Architecture Platform (RIAPS)

RIAPS [2] is a software platform: an 'operating system' for Smart Grid software, not unlike Android for smartphones that supports the construction and operation of distributed applications ('apps') that run on a network of field computing devices. It is based on a message-oriented software component model, where the applications are constructed from a network of interacting components (similar to 'agents', but more tuned for real-time performance) that exchange messages, but also communicate with local power system devices (e.g., PMUs, inverters, breakers, relays, etc.). RIAPS runs on small, inexpensive, embedded computing devices, and provides several services for messaging, dynamic application composition, resource management, distributed coordination among dispersed components, and fault tolerance. It also provides a foundation for strong cyber security, including encryption and Mandatory Access Control (MAC) for applications. RIAPS has a software development kit, including tools for application deployment and management, and is available under an open-source license. Figure 6 shows the software platform's architecture.

RIAPS consists of two sets of software modules: (1) the component framework that includes support libraries to build distributed apps, and (2) the platform managers that includes service programs that assist with the remote installation, operation, security, and management of the apps.

The RIAPS component framework is a software layer above an underlying operating system (Real-time enabled Linux), and can support a variety of applications that implement various functions, like power management, secondary level microgrid control, etc. What RIAPS offers to developers is a set of services that help with building resilient, secure distributed applications. Each computing host ('RIAPS node') in a RIAPS network runs a copy of the platform, as shown on Figure 6.

The functions of distributed applications arise from the interactions among computing nodes. Interactions are implemented as message exchanges, through which the application components share data and salient events. Each node is responsible for its own control actions, but it works with the other nodes to achieve overall control objectives.

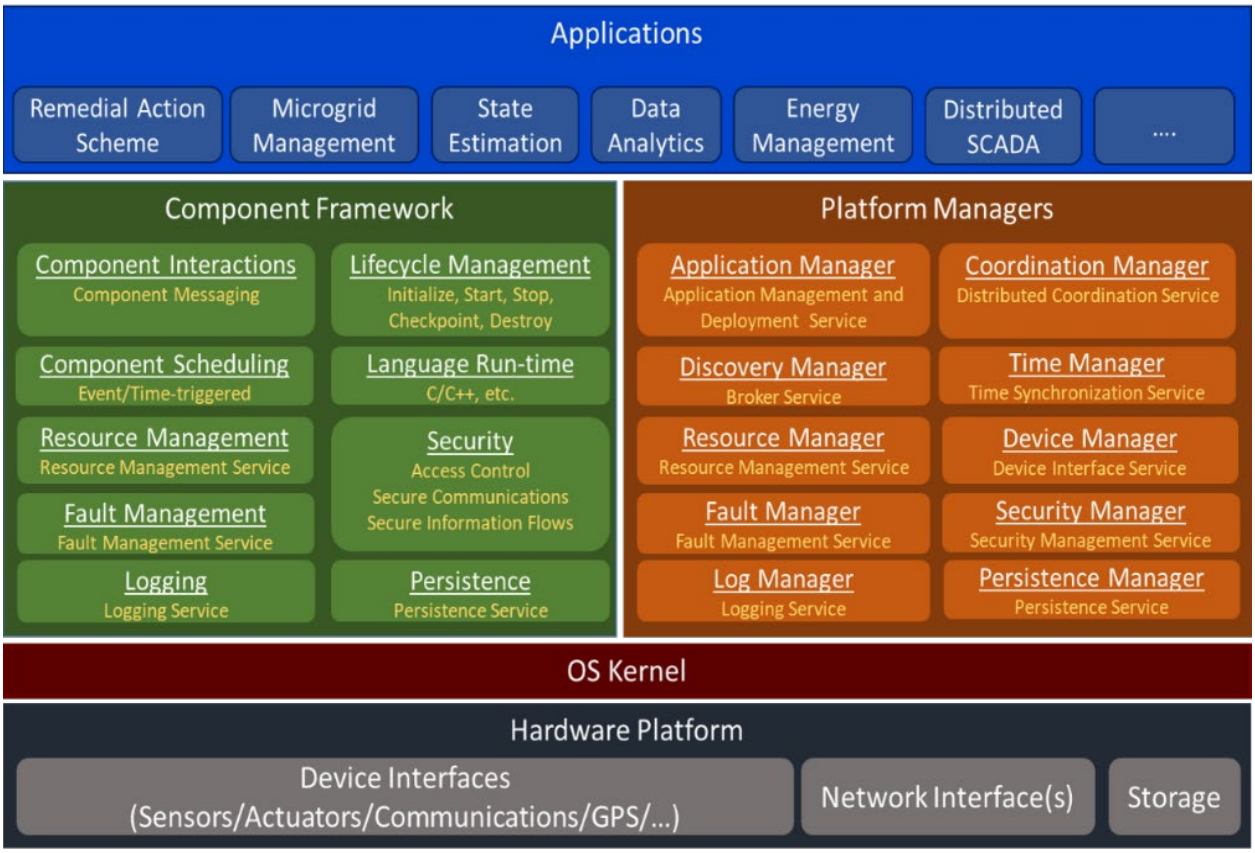

Figure 6. RIAPS Architecture

There are several features in RIAPS to facilitate this paradigm, including support for fault detection, isolation, and recovery, high-precision clock synchronization across the network, real-time scheduling, and encrypted and authenticated communications.

2.1.2 Distributed Microgrid Controller

The microgrid controller algorithm manages (1) islanded operation, including energy management functions and emergency dispatch order functions based on the energy management goals defined by the use case; (2) grid connected operation, including demand response, and methodologies to reduce demand charges, based on the information provided about the site; and (3) transition functions that ensure planned and unplanned seamless transition from grid connected to islanded operation and back to grid connected mode. Thus, the microgrid controller design provides for all the functional requirements that ensure a technically sound operation of the microgrid, per the IEEE 2030.7 standard. The standard defines the microgrid operating modes and transitions among them, as shown on Figure 7.

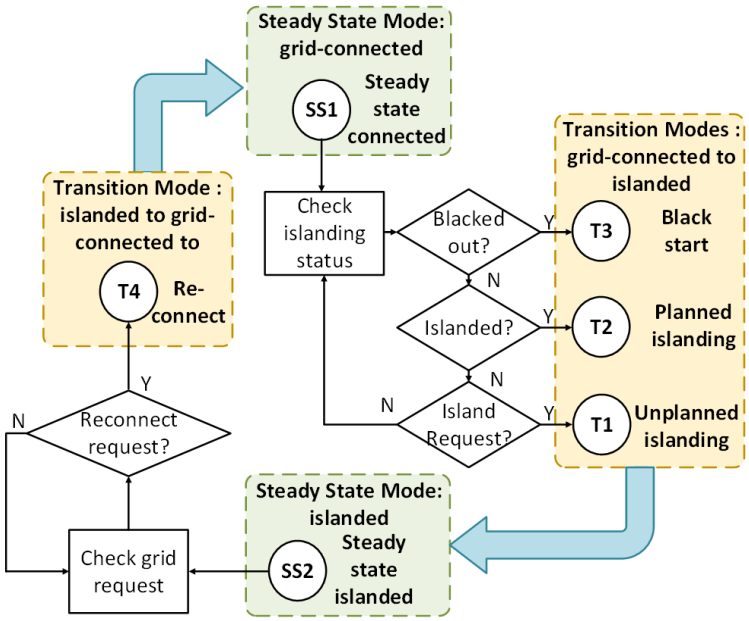

Figure 7. MG Operation Modes per IEEE Std. 2030.7

Conventional microgrid controllers implement these functions using a centralized architecture, where each DG can be individually monitored and controlled, but the actual control function is implemented in a single, central controlling computer. This solution leads to potential problems with fault-tolerance: the centralized controller is a single point of failure. Furthermore, the network round-trip time between the DG and the centralized controller can be unacceptable.

To address these shortcomings, IMCP implements these functions in a fully distributed architectures as illustrated in Figure 8. In this architecture, each DG has its own local controller, which exchanges data with other controllers connected to the same network. Each local controller is capable of operating independently, although with degraded performance, even if connectivity to the network is lost. This provides resilience for the overall system. If the local controller is connected to its peers, coordination is possible, and the system is operating with high performance. The distributed microgrid controller IMCP has been implemented as a RIAPS 'application'.

The microgrid controller application coordinates a set of low-capacity distributed generators (DG) to achieve a system-level goal. As a power system, this is different from many state-of-the art microgrid implementations where one large energy storage unit has sufficient capacity to smooth out the system dynamics and acts as the "grid forming" unit in islanded mode. In islanded operating mode and for microgrid synchronization to the main grid, the DG assets coordinate to proportionally share the real and reactive power system load while restoring the microgrid voltage and frequency and eliminating the amplitude and phase differences between the voltages on either side of the relay at the point of interconnection. The approach uses pinning-based consensus algorithms to coordinate among the DG assets. Other applications use a similar approach to coordinate assets in neighboring microgrids to achieve seamless connection and islanded operation of adjacent microgrids and thus supply critical loads when facing system contingencies or fault conditions. These distributed applications make use of the consensus-based algorithms implemented on the RIAPS platform, the platform group formation and time synchronization functionalities.

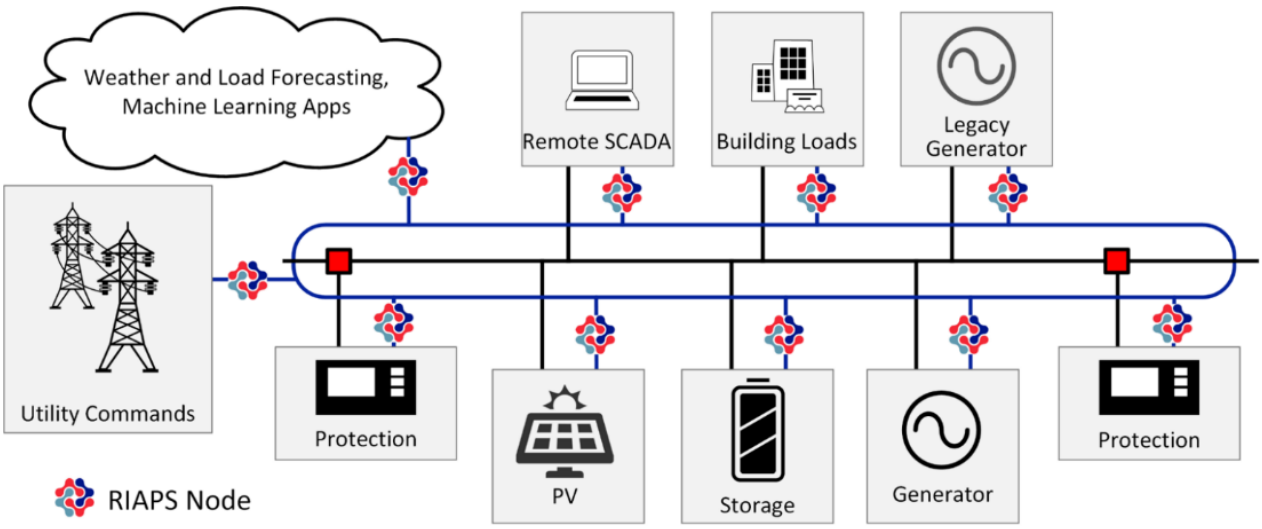

Figure 8. Distributed Microgrid Control Application: IMCP Built with RIAPS

The IMCP was designed to be a highly configurable software system. Each device interface that connect the controller software to actual physical inverters, relays, gensets, etc., is customizable to specific device addresses accessible via the Modbus protocol. The controller algorithms coefficients, i.e., the controller gains are also customizable for specific functions. Furthermore, the IMCP has been extended with a simple graphical user interface that allows the visualization of the one-line diagram of the microgrid's circuits, and these user interface can also be customized to specific data points, sensed or controlled, available in the actual instance of the IMCP application, for a given microgrid.

The benefit of the approach is in the reusability of the algorithms and the interfaces across many DoD installations and microgrid use cases though the development of highly configurable and reusable software components. We envision that controllers for new microgrid configurations can be inexpensively constructed by composing ('wiring') and parameterizing existing software components. Our approach builds on an open-source platform that allows for easy integration of state of the art and legacy equipment into a microgrid management system. Different from other commercial offerings, the developed solution is (1) fully open source - allowing for applications, component interfaces, energy management and power management algorithms to be used across any number of installations and use cases; (2) the approach is distributed - allowing for simple system scaling, and reconfiguration, as the microgrid grows, or as the boundaries of the microgrid and its critical loads move. While existing state of the art solutions are designed to be closed to the user and are typically designed to be centralized. The life cycle cost advantage comes from the reusability of the interfaces and algorithms.

2.1.3 IMCP Implementation Details

The work under this project developed a MG controller that seamlessly integrates disparate algorithms that implement different microgrid functions in distributed manner.

- In the IMCP framework, the dispatch and transition functions, defined by IEEE Standard 2030.7, are implemented using dedicated components in a distributed manner.

A component is defined as an abstract unit that provides the user-defined function by storing its local states and exchanging information with other components. In practice, a component can be implemented as a software thread.

- To implement the dispatch functions, we identify a set of distributed algorithms that are implemented in a microgrid computational component. The distributed algorithms are designed to be consensus-based, where each type of the assets (e.g. DER or relay) acts in a singular and consistent way for a given use case, regardless of the underlying properties of the asset. Some of these algorithms were prototyped under an ARPA-E project, but they were not designed to act as an integrated MG controller, which is the work that was performed under this project.
- To implement the transition function, a state machine component is implemented on every DER node, resulting in a distributed state machine implementation. The local states of individual nodes can be unsynchronized, i.e., they have different states, under abnormal conditions. Methods are provided to resolve the unsynchronized states.
- The IMCP controller can also control and manage networked, i.e., interconnected microgrids. Tie-lines can connect and disconnect separate microgrids, and the controller maintains overall power dispatch and transition functions.
- The IMCP controller does not require a primary DER with a large capacity or distinguish between the leader DERs and the follower DERs. All DERs have the same control priority regardless of their ratings and locations; they execute the same algorithm for a given MG state. With a distributed implementation of the state machine, all DERs together determine the MG state. Therefore, the framework provides a fully distributed implementation of the dispatch and transition functions defined by IEEE Standard 2030.7.

The controller is implemented a set of software components that are executed on different computing nodes and interact with each other by sending and receiving messages. The actual IMCP implementation framework is summarized in Figure 9. The messages used by the framework are listed in Table 2. The framework consists of the state machine component (SMC) that keeps track of the current MG use case, the microgrid computational component (MCC) that executes state-specific algorithms, the relay control component (RCC) that implements the POI relay logic, and the device I/O component (DIOC) that translates vendor-specific messages into the platform environment in a generic form that is usable by other components.

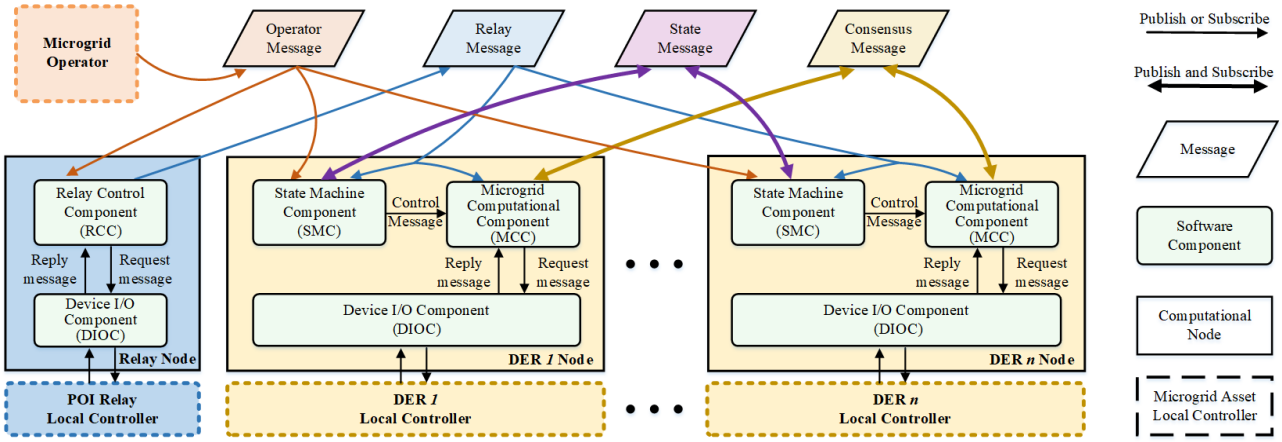

Figure 9. IMCP Implementation Details

Table 2. IMCP Messages

Message	Scope	Producer	Consumer	Information content
operator message	global	operator	SMC, RCC	planned islanding or reconnecting request and POI power command
relay message	global	RCC	SMC, MCC	POI relay measurements, e.g., active power, reactive power, frequency difference, voltage difference, and angle difference
consensus message	global	MCC	MCC	consensus variables, e.g., per unit active power, per unit reactive power, incremental cost, per unit voltage
state message	global	SMC	SMC	local state
control message	local (DER node)	SMC	MCC	majority state and operator's request
request message	local (on DER node)	MCC	DIOC	request DER measurements or send control variable ω_i and E_i
reply message	local (on DER node)	DIOC	MCC	feedback DER measurements or confirmation
request message	local (on Relay node)	RCC	DIOC	read POI relay measurements or send open/close command
reply message	local (on Relay node)	DIOC	RCC	feedback POI relay measurements or confirmation

Below the specific components are explained.

2.1.3.1 State Machine Component (SMC)

The goal of SMC is to determine the MG use case. During each time step, the SMC:

- Determines its local state based on a state machine logic;
- determines the majority state by a majority vote among the local states of all the DERs.

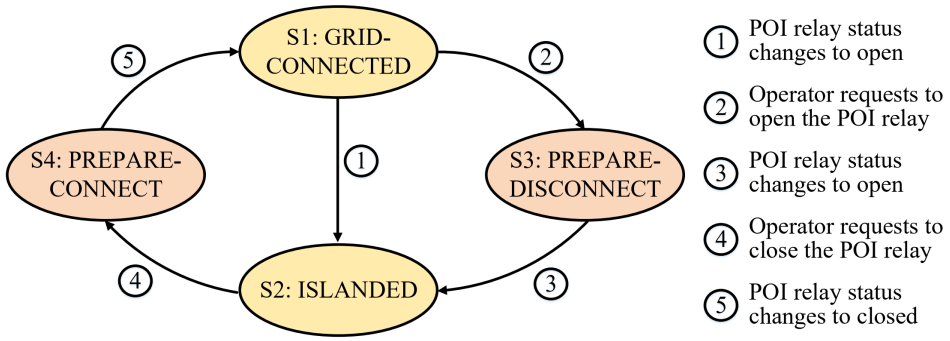

Figure 10. State Machine Logic

The state machine logic for the SMC is shown in Figure 10. The inputs are the POI relay status and the islanding/reconnecting request. To get the inputs, the SMC subscribes to the relay message and the operator's message. The states are described in detail as follows.

- *S1, GRID-CONNECTED* state, corresponds to SS1 grid-connected operation. In this state, the POI power control algorithm is active. From this state, the SMC will enter S2 if the POI relay is open unintentionally (i.e., unplanned islanding). The SMC can also transition to S3 before intentionally opening the POI relay (i.e., planned islanding), which is triggered by an islanding request from the operator.
- *S2, ISLANDED* state, corresponds to SS2 islanded operation. In this state, the frequency and voltage regulation algorithm are active. From this state, the SMC will enter S4 if a reconnecting request from the operator is received. There is no direct transition from S2 to S1, which means that the voltages on the two sides of the POI relay must be synchronized before the MG is reconnected to the grid.
- *S3, PREPARE-DISCONNECT* state, corresponds to T2 planned islanding. In this state, the relay power control algorithm is active. From this state, the SMC will transition to S2 once it receives the POI relay message that confirms that it is open.
- *S4, PREPARE-CONNECT* state, corresponds to T3 reconnecting. In this state, the re-synchronization algorithm is active. From this state, the SMC will enter state S1 once it receives the POI relay message that confirms that it is closed.

All the DER nodes have the same SMC and inputs, resulting in a distributed state machine implementation. Under normal operation, the SMCs of all DERs have the same local state which is a local estimate of the MG use case. However, as a distributed implementation, the SMCs on different nodes could have unsynchronized states under abnormal conditions and destabilize the MG. For example, during unintentional islanding, if one DER node fails to receive the relay message, the SMC on this node stays in S1 while others enter S2. The DER staying in S1 will activate algorithm to regulate the POI power, which is impossible since the MG is islanded.

To resolve the unsynchronized states, a majority state is used. Each SMC publishes its local state under the state message and subscribes to the state message as well. As a result, the SMC on each DER node can receive the local states of all the DERs. A majority vote is held among the local states to determine the majority state, which is sent to the MCC to determine the active distributed algorithm.

2.1.3.2 Microgrid Computational Component (MCC)

At the core of the MCC is a function that is triggered at a selected frequency, which determines the time step of the distributed algorithms. During each time step, the MCC:

- communicates with the DIOC to collect the latest measurements;
- executes the selected distributed algorithm depending on the state received from the SMC;
- sends the control variables to the DIOC and publishes consensus variables.

The collected measurements include the DER active power, reactive power, frequency, voltage, and any other variables that are used by the distributed algorithms. The MCC subscribes to the relay message to get the POI measurements, which are used by distributed control algorithm. In this implementation, three algorithms are considered:

Algorithm 1: POI power control for grid-connected operation: When the MG is grid-connected, the power exchange at the POI should follow a command from the grid. While all the DERs coordinate to control the POI power exchange, the power output of individual DERs can be dispatched in several ways depending on the desired performance. The implemented IMCP algorithm dispatches the power output proportionally to the DERs' rating, i.e., all the DERs have the same per unit active and reactive power output, as described in [4]; this implementation also supports proportional power sharing and POI power control. Another commonly used dispatch method compatible with IMCP implementation is described in[5], which implements the distributed economic dispatch algorithm. This implementation considers the economics of each generator operation in the implementation.

Algorithm 2: Frequency and voltage regulation for islanded operation: When the MG is in islanded operation, the DERs regulate the MG frequency and voltage magnitude to the rated values. In the steady state, algorithms regulate the MG frequency and average voltage to their rated values while keeping the power output of the DERs proportional to their ratings. The implemented IMCP algorithm follows the formulation described in [6].

Algorithm 3: POI power control for planned islanding: when the MG is grid-connected, it may be desired to open the POI relay to bring the MG into islanded operation. Before sending the command to open the relay, the power flow through the relay should be minimized to limit the transient introduced by opening the relay. This algorithm can be seen as a special case of Algorithm 1, setting the active and reactive power reference to zeros. In the steady state, the POI power is regulated to zero, and the power sharing among the DERs is proportional to their ratings.

Algorithm 4: Re-synchronization for reconnecting: When the MG is in islanded operation, it may be desired to close the POI relay to bring the MG back into grid-connected operation. Before closing the relay, the voltages on both sides of the relay should be synchronized. In the steady state, the voltages on the two sides of the relay are synchronized, and the power sharing among the DERs is proportional to their ratings. The implemented IMCP algorithm follows the implementation described in[7].

For all algorithms, the MCC of each DER requires the consensus variables (e.g., per unit active power, per unit reactive power) from other DERs, which is achieved by subscribing to the consensus message. In S1 and S2, the MCC executes Algorithm 1 and Algorithm 2, respectively. In S3 and S4, the MCC executes Algorithm 3 and Algorithm 4, respectively. The calculated control variables ω_i and E_i are sent to the DIOC. The consensus variables are published under the consensus message, which will be received and used by the DERs' MCCs in the next time step.

2.1.3.3 Relay Control Component (RCC)

During each time step, the RCC on the POI relay node

- communicates with the DIOC on the relay node to collect the latest measurements.
- determines whether the condition to close/open the POI relay is satisfied or not.
- sends the close/open command to DIOC on the relay node if necessary and publishes the latest measurements.

The collected measurements include POI relay status, active power and reactive power flowing through the relay, frequency difference, voltage magnitude difference, and phase angle difference between the two sides of the relay, and any other POI relay variables that are used by the distributed algorithms. The RCC subscribes to the operator message to know if there is any request. If the MG is grid-connected and a planned islanding request is issued, the RCC checks whether the condition to open the relay is satisfied, i.e., active power and reactive power flowing through the relay are smaller than the pre-defined thresholds. If the MG is islanded and it is requested to reconnect to the grid, the RCC checks whether the condition to close the relay is satisfied, i.e., the frequency difference, voltage magnitude difference, and phase angle difference are smaller than the pre-defined thresholds. If the corresponding condition is satisfied, the RCC sends the open/close command to the DIOC on the relay node. The RCC also publishes the relay measurements under the relay message.

2.1.3.4 DER Device I/O Component (DDC)

The DDC uses IEEE 1547 Standard protocols (e.g. Modbus, DNP3) to collect measurements from and send commands to the DER's local controller. The DER behavior is encapsulated into the DDC such that the MCC only needs to communicate with the DDC. By doing so, the MCC is isolated from the communication link and protocol used between the DDC and the DER's local controller. As a result, the MCC is the same for all the DERs no matter which protocol is used, i.e., the MCC is re-usable for all DERs regardless of their underlying property.

2.1.3.5 Device I/O Component (DIOC)

The DIOC communicates with the end device's local controller using a protocol supported by that device (e.g. Modbus, DNP3, IEC 61850 GOOSE). The device behavior is encapsulated into the DIOC such that other components in the framework only need to communicate with the DIOC. As a result, other components are isolated from the communication link and protocol used between the DIOC and the end device, making them reusable for any device, regardless of the underlying specifics (e.g., manufacturer, the protocol used, etc.).

2.1.4 MG use cases with the proposed framework

In the following, sequence diagrams are used to illustrate how the components in the proposed framework interact with each other to support different MG use cases.

2.1.4.1 Grid-connected operation

Figure 11 shows the sequence diagram for the grid-connected operation. The MG operator publishes the operator message that contains the reference POI power, and no islanding request is issued. The DIOC on the relay node communicates with the POI relay to get the latest measurements and sends them to the RCC. The RCC further publishes the measurements under the relay message.

The SMC subscribes to the relay message and the operator message to determine the current state. As the POI relay is closed and no islanding request is issued, the SMC determines that the current state is S1. The current state and the reference POI power received from the operator message are packaged and published as the control message, which is received by the MCC. In S1, the MCC runs Algorithm 1 to regulate the POI power to its reference value. The calculated control variables ω_i and E_i are sent by the MCC to the DIOC.

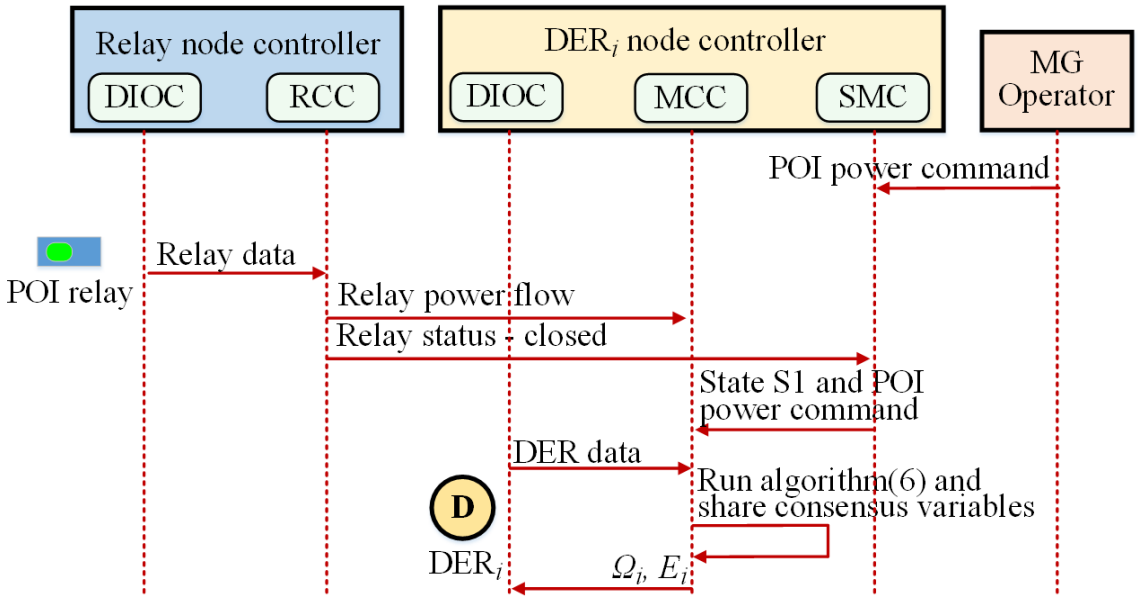

Figure 11. Grid-connected Operation

2.1.4.2 Unplanned islanding

Figure 12 shows the sequence diagram for the unplanned islanding. It is assumed that the generation capacity exceeds the loads after the unplanned islanding event. Initially, the MG is in grid-connected operation. At one moment, the POI relay is opened without any islanding request. The relay status is published under the relay message. After the SMC receives the relay message, the state transitions from S1 to S2. In S2, the MCC selects Algorithm 2 to regulate the frequency and voltage of the islanded MG.

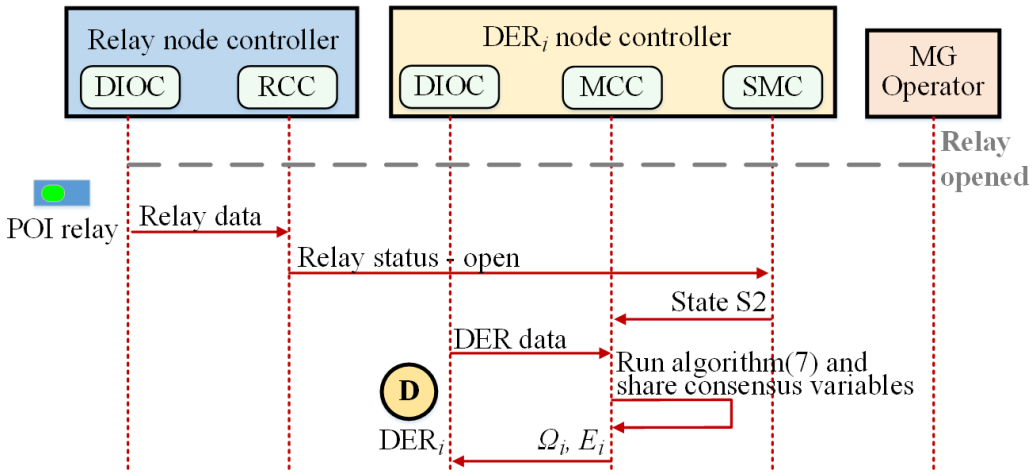

Figure 12. Unplanned Islanding

2.1.4.3 Planned islanding

Figure 13 shows the sequence diagram for the planned islanding. The MG is in grid-connected operation until the MG operator publishes the operator message that contains the islanding request. After the SMC receives this request, the state transitions from S1 to S3. In S3, the MCC selects Algorithm 3 to regulate the POI power to zero.

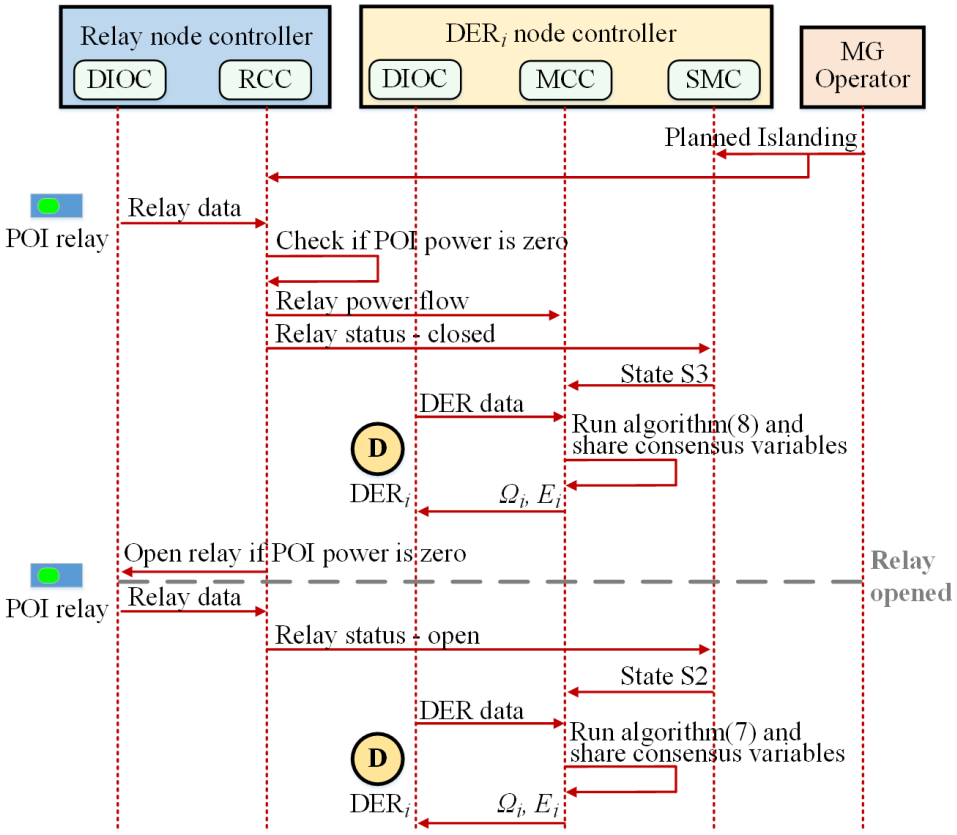

Figure 13. Planned Islanding

The RCC on the POI relay node subscribes to the operator message. After it receives the islanding request, it constantly checks if the active and reactive power at the POI are smaller than the pre-defined thresholds. Once the condition is met, the RCC sends an open command to the DIOC on the relay node, which further sends it to the POI relay's local controller. When the POI relay status changes from closed to open, the SMC receives this change and transitions from S3 to S2. In S2, the MCC selects Algorithm 2 to regulate the frequency and voltage of the islanded MG.

2.1.4.4 Islanded operation

Figure 14 shows the sequence diagram for the islanded operation. If no reconnecting request is received from the operator, the SMC determines that the current state is S2. In S2, Algorithm 2 is used to regulate the frequency and voltage of the islanded MG.

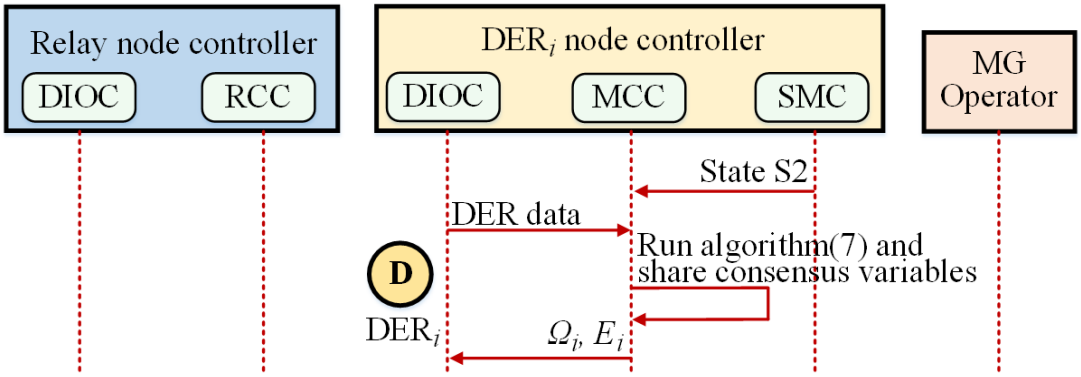

Figure 14. Islanded Operation

2.1.4.5 Reconnecting

Figure 15 shows the sequence diagram for reconnecting. The MG is in islanded operation until the MG operator publishes the operator message that contains the reconnecting request. When the SMC receives this request, the state transitions from S2 to S4. In S4, the MCC selects algorithm 4 to eliminate the frequency difference, voltage magnitude difference, and phase angle difference between the two sides of the POI relay.

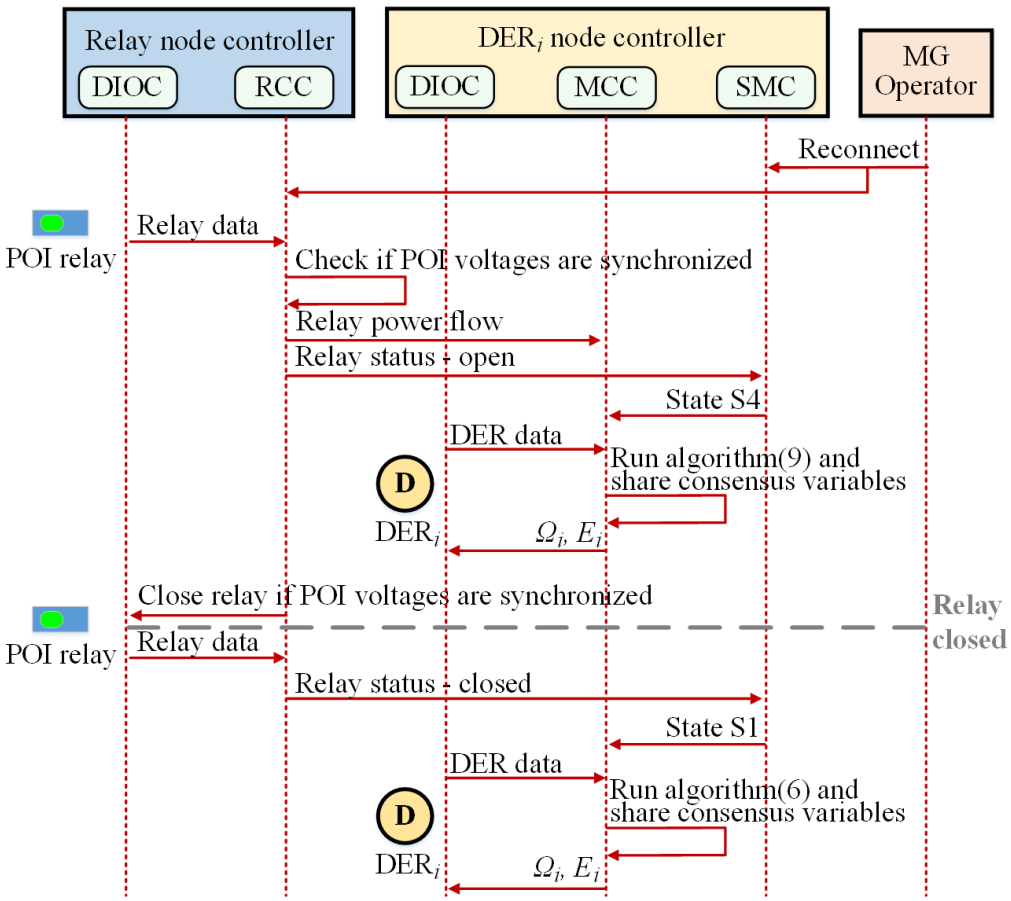

Figure 15. Reconnecting

After the RCC on the POI relay node receives the reconnecting request, it constantly checks if the frequency difference, voltage magnitude difference, and phase angle difference are smaller than the pre-defined thresholds. Once the condition is met, the RCC sends a close command to the DIOC on the relay node, which further sends it to the POI relay's local controller. When the POI relay status changes from open to closed, the SMC transitions from S4 to S1. In S1, the MCC switches to Algorithm 1 to regulate the POI power as the MG is in the grid-connected operation.

2.2 TECHNOLOGY DEVELOPMENT

The project has executed the following technology development activities.

1. Extension, installation, and operating of the Banshee microgrid simulation model at the HIL lab. All the IMCP control algorithms were tested in an HIL environment, where an OPAL-RT real-time power system simulator was used. In this activity, the Banshee model was extended with additional DER components to evaluate the performance of the IMCP on more challenging scenarios. The modification introduced to the Banshee Microgrid topology are shown in Figure 4. Each introduces resource in the microgrid had to be modeled in the HIL environment and had to be interfaced tot eh hardware controller in the loop, which consists of a Texas Instruments F28377S microcontroller and a beagle bone black running he RIAPS platform.

2. Design and implementation of RIAPS Modbus interface software components for the IMCP. A new software component has been developed to interface RIAPS application code to arbitrary DER-s that implement the Modbus protocol. This was necessary because the Banshee model used this protocol for communication between the control algorithms and the (simulated) hardware elements.
3. Design and implementation a new RIAPS software component for Finite-State Machines (FSM). The software component implements a configurable FSM, that was used to implement the fault-tolerant transition logic inside the IMCP application software.
4. Design and implementation of the entire IMCP application software. This effort focused on implementing the abstract algorithms in actual software code that performs that various controller functions. The resulting implementation is a fully distributed, componentized software, that runs on the RIAPS platform.
5. Design and implementation of an MQTT interface component for RIAPS. This software component can connect RIAPS applications to other systems that can interact with the MQTT broker. MQTT is an industry-standard communication system for interconnecting computers in an industrial environment.
6. Design and implementation a Graphical User Interface (GUI) for testing. This interface was necessary for demonstration purposes. It shows the Banshee network diagram, and it allows an operator to exercise the various demonstration scenarios. Figure 16 shows the interface in operation.

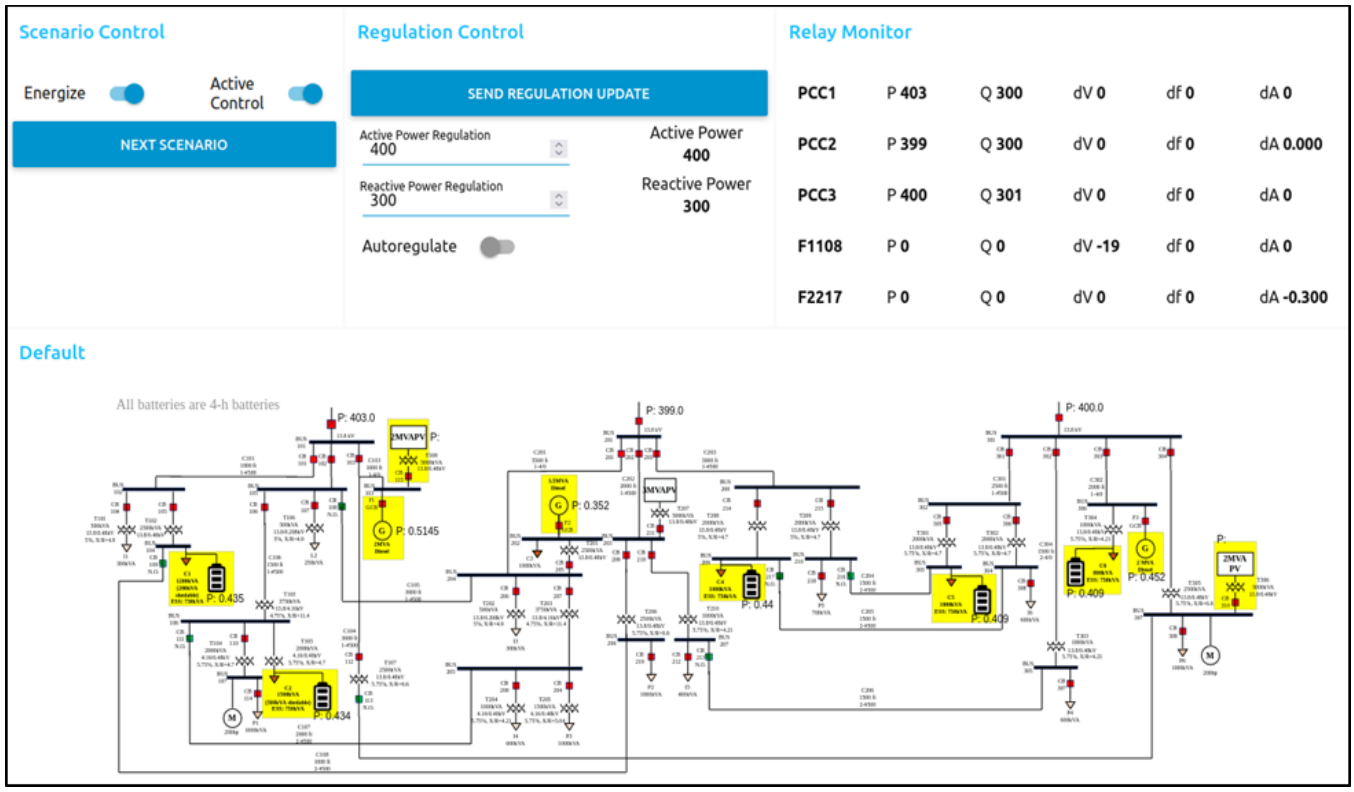

Figure 16. Test Graphical User Interface

7. Developing and executing tests on the HIL platform. The project has developed a collection of test scenarios for evaluating the performance of the IMCP controller, as well as for cyber-security testing. The tests were executed on a realistic, distributed, embedded hardware devices (Beaglebone Black evaluation boards), connected to a real-time, high-fidelity power system simulator (OPAL-RT). The tests were designed to demonstrate that the controller meets the criteria specified in the IEEE standards.

2.3 ADVANTAGES AND LIMITATIONS OF THE TECHNOLOGY

The IMCP is a complete microgrid controller with a novel architecture: a fully distributed system. It implements all the microgrid control functions specified in the IEEE standard, and it can be implemented on low-end embedded computer devices (if they have the right I/O interfaces.

The advantages of the technology include:

- Distributed controller architecture, where each DER node has its own controller. Because there is no 'central' controller computer, there is no single point of failure.
- Fault tolerance: even if a DER node gets disconnected from the communication network, its controller maintains control based on the last communications received. When the node gets re-connected, the controller recovers.
- Robustness: the underlying software platform RIAPS provides a number of services to ensure robustness and security. These include: high-precision time synchronization, automatic fault detection and recovery (for specific cases), and secure communications to preserve confidentiality and integrity of data and the availability of the system.
- Cost: the IMCP and the software platform it is running on: RIAPS are open source, distributed with an open source license (Apache2). Businesses can use the software and customize, extend, and use it without restrictions. The embedded computing devices used are very cost-effective as well.

The limitations of the technology include:

- Due to limitations in time-domain performance of the software, the controller implements only Level 2 microgrid control functions: power dispatch and transition control. High-frequency, sub-millisecond-level control is not possible. Such controls are typically implemented on special purpose DSP devices.
- The controller does not implement protection functions that would require 10 msec-level response times. Such functions are typically implemented using dedicated, fast relays.
- The technology includes only the software for the microgrid controller, for a complete field installation several other technologies are needed: industrial-quality embedded computers, a robust local area network, dedicated interfaces to the actual DERs, and including all the material and labor to implement the system.

3.0 PERFORMANCE OBJECTIVES

3.1 POWER SYSTEM PERFORMANCE METRICS AND OBJECTIVES

The table below summarizes the electrical performance objectives of the IMCP system. Allowable voltage, frequency and rate-of-change-of-frequency (ROCOF) metrics are listed in the Table. They list the allowable operating bands, which are evaluated on all buses throughout the transition process. The metrics are derived from the IEEE 1547 standard ride-through requirements for DER in Category II.

Variable	Allowable Range
Voltage	$0.88 \leq V \leq 1.10\ p.u.$
Frequency	$58.8 \leq f \leq 61.2\ Hz$
Rate of change of Frequency	$RoCoF \leq 2\ Hz/s$

Performance Objective	Metric	Data Requirements	Success Criteria
GRID CONNECTED			
Compliance with Institute of Electrical and Electronics Engineers (IEEE) 2030.8 for grid-tied operation	Follow DSO commands for power flow at PPC including: PQ dispatch, following kW/Hz and kVAr/Volt droop during voltage/ frequency events, PF command.	V, f, P, Q, settling time, overshoot, and SS values at all buses including PCC.	Commands followed within 5% without violating component ratings or deviating from allowable voltage or frequency range.
GRID TO ISLAND TRANSITION			
Compliance with IEEE 2030.8 for planned transition to stable microgrid	Seamlessly disconnect from the main grid in response to a command from the DSO.	V, f, P, Q, settling time, overshoot, and SS values at all buses including PCC.	Seamless transition from grid connected to islanded mode at prescribed time. Voltage and frequency variation within allowable bands throughout the transition process at all buses in accordance to IEEE 1547.
Compliance with IEEE 2030.8 for unplanned transition to stable microgrid	Seamlessly disconnect from the main grid when a fault occurs on the main grid.	V, f, P, Q, settling time, overshoot, and SS values at all buses including PCC.	Seamless transition from grid connected to islanded mode at prescribed time. Voltage and frequency variation within allowable bands throughout the transition process at all buses in accordance to IEEE 1547.
ISLANDED OPERATIONS			
Critical load support in compliance with IEEE 2030.8 steady state islanding requirements	Maintain power balance within the islanded microgrid and shed low priority loads to maintain power supply to critical loads.	V, f, P, Q, settling time, overshoot, and SS values at all buses including PCC.	Maintain power supply to all critical loads with voltage and frequency variation within allowable bands throughout the islanded operation.
Critical load support in case of DER failures	Maintain power balance within the islanded microgrid in case of DR failure.	V, f, P, Q, settling time, overshoot, and SS values at all buses including PCC.	Maintain power supply to all critical loads with voltage and frequency variation within allowable bands throughout the islanded operation.
ISLAND TO GRID TRANSITION			
Synchronization: autonomously recognize grid restoration and initiate synchronization of the microgrid	Seamlessly connect to the main grid after grid restoration.	V, f, P, Q, settling time, overshoot, and SS values at all buses including PCC.	Seamless transition from islanded to grid connected mode at prescribed time. Voltage and frequency variation within allowable bands throughout the transition process at all buses.

3.1.1 Definitions for Performance Objectives

1. Grid Tied Operation
   1.1. Name and Definition: Compliance with Institute of Electrical and Electronics Engineers (IEEE) 2030.8 for grid-tied operation
   1.2. Purpose: The purpose of this performance metric is to demonstrate the platform's ability to coordinate the response of multiple resources to a grid command.
   1.3. Metric: Follow DSO commands for power flow at PPC which includes PQ dispatch, following kW/Hz and kVAr/Volt droop during voltage/frequency events and PF command.
   1.4. Data: V, f, P, Q, settling time, overshoot, and SS values at all buses including PCC. The data will be collected from the OPAL-RT simulator and will be stored in a MATLAB file for further processing. Data to be collected will include the V, f, P, Q at the POI at buses 101, 201, and 301, and at all the DGs in the system, to show power sharing in accordance with the power sharing rules. In addition, the simulated commands from the DSO will also be logged when applicable. The collected data will show that the DSO command is followed and that the DGs are sharing power in accordance with the power sharing rules.
   1.5. Success Criteria: Commands followed within 5% without violating component ratings or deviating from allowable voltage or frequency range.

2. Planned Grid to Island Transition
   2.1. Name and Definition: Compliance with Institute of Electrical and Electronics Engineers (IEEE) 2030.8 for planned transition to stable microgrid.
   2.2. Purpose: The purpose of this performance metric is to demonstrate the platform's ability to support a seamless disconnect from the main grid in response to a command from the DSO.
   2.3. Metric: Disconnect from the main grid in response to a command from the DSO while maintaining the voltage and frequency in the allowable range (per IEEE 1547) within the MG.
   2.4. Data: V, f, P, Q, settling time, overshoot, and SS values at all buses including PCC. The data will be collected from the OPAL-RT simulator and will be stored in a MATLAB file for further processing. Data to be collected will include the V, f, P, Q at the POI at buses 101, 201, and 301, and at all the DGs in the system to show power sharing in accordance with the power sharing rules. In addition, the simulated commands form the DSO will be logged where applicable. The collected data will show that the IMCP responds to the DSO command by bringing the power flow through the POI relay to zero prior to the planned islanding event. As a result, the voltage and frequency deviations due to the operation of the POI breaker will be minimal and in compliance with the relevant standards as described in the success criteria. Throughout the process, the power sources within the MG will share power proportionally, in accordance with the power sharing rules defined by the control algorithm.

2.5. Success Criteria: Seamless transition from grid connected to islanded mode at prescribed time. Voltage and frequency variation within allowable bands throughout the transition process on all buses in accordance with IEEE 1547. Voltage at load buses will conform to the CBEMA/ITIC curves as below.

3. Unplanned Grid to Island Transition

3.1. Name and Definition: Compliance with Institute of Electrical and Electronics Engineers (IEEE) 2030.8 for unplanned transition to stable microgrid.

3.2. Purpose: The purpose of this performance metric is to demonstrate platform's ability to support seamless disconnect from the main grid when a fault occurs on the main grid.

3.3. Metric: Disconnect from the main grid when a fault occurs on the main grid while maintaining the voltage and frequency in the microgrid within the allowable range per IEEE 1547.

3.4. Data: V, f, P, Q, settling time, overshoot, and SS values at all buses including PCC. The data will be collected from the OPAL-RT simulator and will be stored in a MATLAB file for further processing. Data to be collected will include the V, f, P, Q at the POI at buses 101, 201, and 301, and at all the DGs in the system to show power sharing in accordance with the power sharing rules. The collected data will show the voltage and frequency transients on various buses when an unplanned islanding event occurs. The data will also show the load shedding and generator setpoint changes and dynamics in response to the islanding event.

3.5. Success Criteria: Seamless transition from grid connected to islanded mode at prescribed time. Voltage and frequency variation within allowable bands throughout the transition process at all buses in accordance with IEEE 1547.

4. Critical Load Support in Islanded Operating Mode

4.1. Name and Definition: Critical load support in compliance with IEEE 2030.8 steady state islanding requirements

4.2. Purpose: The purpose of this performance metric is to demonstrate the platform's ability to maintain power balance within the islanded microgrid.

4.3. Metric: Maintain power balance within the islanded microgrid and shed low priority loads to maintain power supply to critical loads.

4.4. Data: V, f, P, Q, settling time, overshoot, and SS values at all buses including PCC. The data will be collected from the OPAL-RT simulator and will be stored in a MATLAB file for further processing. Data to be collected will include the V, f, P, Q at the POI at buses 101, 201, and 301, and at all the DGs in the system to show power sharing in accordance with the power sharing rules.

4.5. Success Criteria: Maintain power supply to all critical loads with voltage and frequency variation within allowable bands (per IEEE 1547) throughout the islanded operation.

5. Critical Load Support in Face of DER Failures

5.1. Name and Definition: Critical load support in case of DER failures

5.2. Purpose: The purpose of this performance metric is to demonstrate the platform's ability to support critical loads in case of DER failures

5.3. Metric: Maintain power balance within the islanded microgrid in case of DER failure.

5.4. Data: V, f, P, Q, settling time, overshoot, and SS values at all buses including PCC. The data will be collected from the OPAL-RT simulator and will be stored in a MATLAB file for further processing. Data to be collected will include the V, f, P, Q at the POI at buses 101, 201, and 301, and at all the DGs in the system to show power sharing in accordance with the power sharing rules. Data will show the load shedding sequence that maintains the voltage and frequency at the critical loads within the allowable range. Results will be compared to the base case, without the IMCP.

5.5. Success Criteria: Maintain power supply to all critical loads with voltage and frequency variation within allowable bands (per IEEE 1547) throughout the islanded operation.

6. Synchronization

6.1. Name and Definition: Autonomously recognize grid restoration and initiate synchronization of the microgrid

6.2. Purpose: The purpose of this performance metric is to demonstrate the platform's ability to autonomously recognize grid restoration and initiate synchronization of the microgrid

6.3. Metric: Seamlessly connect to the main grid after grid restoration.

6.4. Data: V, f, P, Q, settling time, overshoot, and SS values at all buses including PCC. The data will be collected from the OPAL-RT simulator and will be stored in a MATLAB file for further processing. Data to be collected will include the V, f, P, Q at the POI at buses 101, 201, and 301, and at all the DGs in the system to show power sharing in accordance with the power sharing rules. Data will show the V,f measurements at either side of the POI relay and how the IMCP eliminated the voltage and frequency mismatch before the relay is closed. The data will show the voltage and frequency at all buses is within the allowable range throughout the process.

6.5. Success Criteria: Seamless transition from islanded to grid connected mode at prescribed time. Voltage and frequency variation within allowable bands (per IEEE 1547) throughout the transition process at all buses.

3.1.2 Cyber-security performance

IMCP is a software application running on a distributed computing platform consisting of several embedded and networked computing devices, which are also connected to power system devices: DERs, inverters, breakers, etc. Given this network architecture, it was necessary to perform cyber-security evaluation on the hardware-software system.

The project has identified a threat model, summarized on Table 3. Note that threats map to specific cyber-security concerns: confidentiality, integrity, and availability.

Table 3. Threat Model

Type of threat	Possible harm	Protection is needed for
Malicious network devices	Observe, possibly modify or disrupt network traffic	*Availability* of resources; confidentiality and integrity of communications
Malicious applications	Interfere with operations, exhaust resources, or physically damage the node or the connected power system	*Confidentiality* and *integrity* of communications, availability of and control over physical resources
Distributed Denial of Service (DDoS) attack	Core applications of the platform are unable to operate	Platform services and remotely deployed and controlled applications to remain *available* even under attack conditions.
Malicious application actors	Unauthorized access to configuration and operational data of another application	*Confidentiality* of data

Assuming these threats, the system is expected to address the threats, as summarized on Table 4 . The table shows concerns related to specific threats, expected attacker actions, and the expected response of the system.

Table 4. Cyber Security expectations

Concern	Attacker action	Expected behavior
Confidentiality	Snoop on network packets	Attacker is unable to decode content
Integrity	Modify and retransmit modified network packets	Modified packet is rejected by recipient
Authenticity	Spoof network packets	Modified packet is rejected by recipient
Availability	Flood network with packets	App detects the problem and acts accordingly, while maintaining (possibly degraded, but acceptable) control performance.

4.0 FACILITY / SITE DESCRIPTION

The testing was performed in a laboratory environment. The environment consisted of a real-time power system simulator (OPAL-RT), a 'RIAPS Control node' PC, a network switch, and a collection of Beaglebone Black embedded computers, as shown on Figure 17.

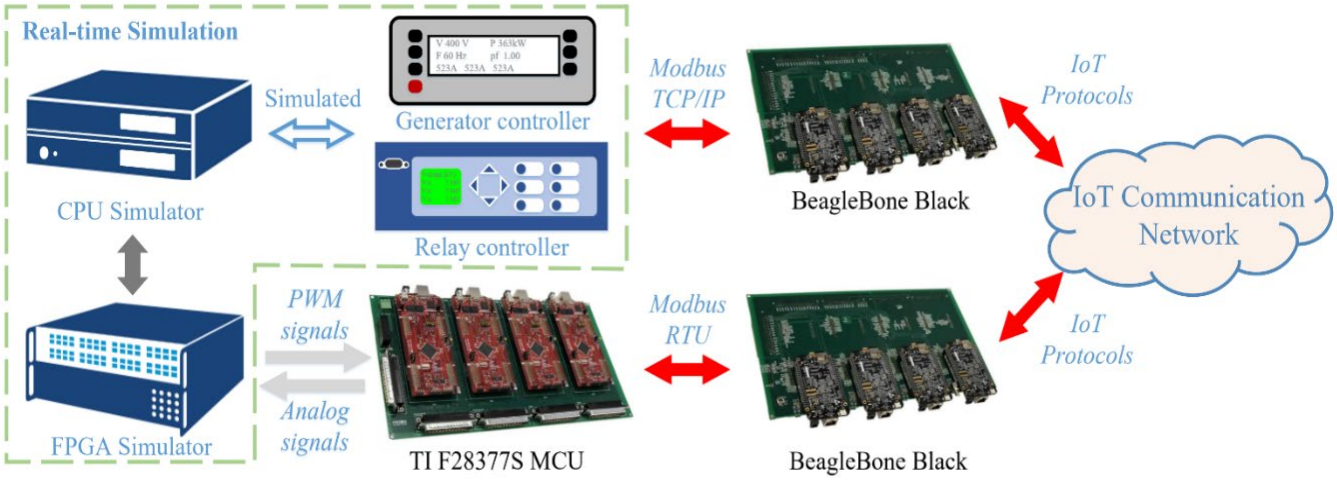

Figure 17. Representation of the Physical Testbed Used for Test the IMCP Platform.

In the HIL testbed OPAL-RT real-time simulator is used to simulate the MG components such as the DERs, line impedances, relays, etc. The switching model of inverters is modeled in the OPAL-RT FPGA-based simulator with a small simulation time step (500 ns) while the non-switching components are modeled in the CPU-based simulator with a larger simulation time step (65 µs).

In the test MG shown in Figure 19, DER1, DER2, DER5, DER6, and DER7 are inverter-based DERs which are controlled by the industry-grade micro-controller units (MCUs) TMS320F28377S from Texas Instruments. The measurements like voltage and current are sampled by the analog-to-digital converters (ADCs) of the MCUs. The MCUs send pulse-width modulated (PWM) signals to the OPAL-RT simulator as gate signals for the simulated inverters. The inverter-based DERs operate in voltage control mode whose control includes the current loop, voltage loop, and droop control that are implemented in the MCUs. DER3, DER4, and DER8 are diesel generators and their local control is implemented in the OPAL-RT simulator. The diesel generators can operate in P-Q or V-F droop control mode.

The POI relays' local control is implemented in the OPAL-RT simulator, including overcurrent, time overcurrent, overvoltage, undervoltage, over-frequency, under-frequency, and rate of change of frequency protection. It also performs a synchronism check that prevents the relay from being closed when the voltages on two sides of the relay are not synchronized.

The IMCP controller was implemented using the RIAPS platform. The hardware for the RIAPS nodes is Beaglebone Black (BBB) embedded computing device. One BBB was assigned to each DER as its computational node. The components SMC, MCC, and DIOC (described in earlier sections and summarized in Figure 9) were implemented as RIAPS components. The components are grouped as a RIAPS DER actor. Each RIAPS component is a single thread while the RIAPS

DER actor is a multi-threaded operating system process. For the inverter-based DERs, the BBBs can communicate with the MCUs through the DIOC using Modbus RTU. For the diesel generators, the BBBs communicate with their simulated local controllers in the OPAL-RT simulator through the DIOC using Modbus TCP/IP.

One BBB is assigned as the POI relay's computational node. The RCC and DIOC are implemented as RIAPS components and grouped as a RIAPS relay actor. The BBB communicates with the relay's simulated local controllers in the OPAL-RT simulator through the DIOC using Modbus TCP/IP.

4.1 FACILITY/SITE LOCATION AND OPERATIONS

The technology has been tested and demonstrated at the FREEDM Center of the North Carolina State University. The lab is equipped with:

- OPAL-RT Real-Time Server - 8 Cores - 3.8 GHz, Intel® Xeon® Gold Processor 2x 4 Cores, 3.8 GHz.
- OP5707-4, OP5700 RCP/HIL Virtex7 FPGA-Based Real-Time Simulator - 4 Cores
- OP5640-I/O, OP5600 v2, RCP/HIL Spartan3
- FPGA Processor and 1/0 Expansion Unit (4U)
- Analog and Digital Input and Output Cards (5 each)
- SEL 451 Distribution Relays (7 units)
- Beaglebone Black Rack (10 units)
- TI C2000 rack (10 units)

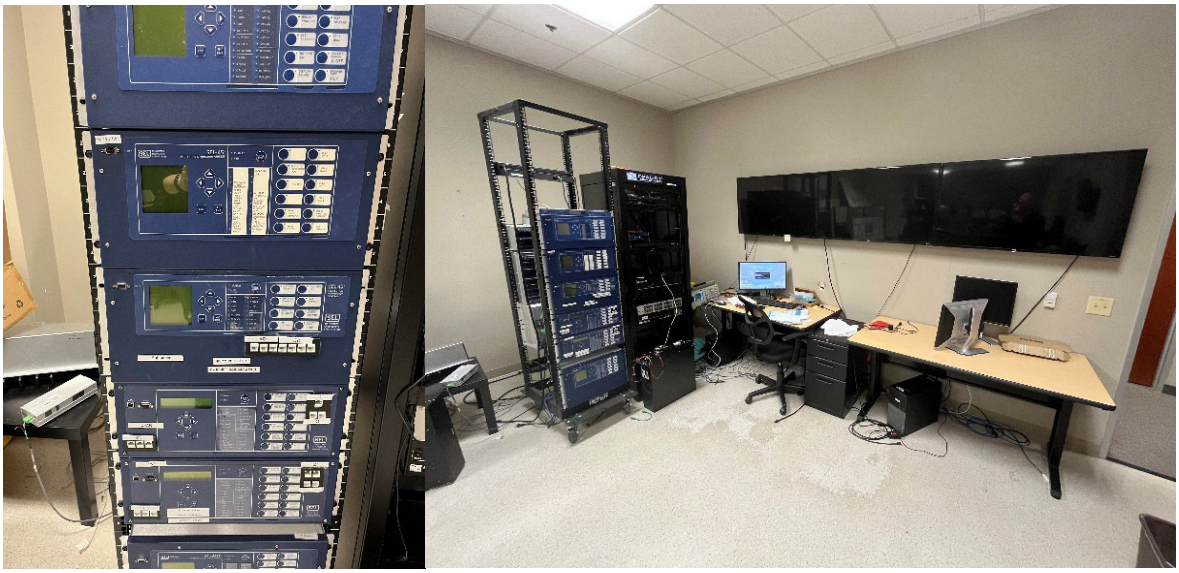

Figure 18. Laboratory Space that Housed the Testbed

The setup is housed at the Future Renewable Electric Energy Delivery and Management Systems (FREEDM) Systems Center, a Center within the college of Engineering at North Carolina State University. FREEDM NSF Engineering Research Center with a research program focusing on the development of physical layer technology needed for the Energy Internet, namely the next-generation distribution grid based on advanced power electronics technology such as the solid-state transformer (SST) and solid-state circuit breaker.

4.2 FACILITY/SITE CONDITIONS

Not applicable: the tests were performed in a university lab.

5.0 TEST DESIGN

5.1 CONCEPTUAL EXPERIMENT DESIGN

To validate the performance and the cyber security features of the IMCP a number of test scenarios have been developed. These test scenarios were executed in an HIL environment where the power system was simulated in a high-performance real-time simulator, and the IMCP controller code was running on a collection networked, embedded computers. This is a closed-loop architecture, where the simulator produces measurement values for and receives control commands from the actual embedded computing devices that run the actual control software. The interface between the two sides with physical connections and the Modbus protocol.

The tests performed were designed to validate that the IMCP meets the performance and cyber-security requirements. Below the various test scenarios are described.

Grid-connected mode test scenarios

These test scenarios evaluate the controller's performance when the microgrid is connected to the utility grid. They demonstrate that (1) the DER-s of the microgrid can be controlled to dispatch power according to their rating (HIL.1), (2) the DER can support the Frequency-Watt and Dynamic Reactive Power Support control mode based on pre-set droop coefficients (HIL.2); (3) the DER-s of the microgrid can be controlled to deliver power at a commanded power factor (PF) (HIL.3); and (4) the system can be reconfigured to have loads shifted from one feeder to another (HIL.4)

Functionality	Simulated initiating event	Command from utility	Success criteria
HIL.1: PQ dispatch	N/A	P and Q command	Value within 5% of rating within 30 seconds (IEEE 1547-2018 clauses 4.4)
HIL.2: Frequency Watt Mode; Dynamic Reactive Power Support	Voltage drops to 0.95pu; frequency change from 0.98 to 1.02pu	Droop coefficients	Value within 5% within 30 seconds (IEEE 1547-2018 clauses 4.4)
HIL.3: PF command	N/A	P and PF command	Value within 5% of rating within 30 seconds (IEEE 1547-2018 clauses 4.4)
HIL.4: Loss of bus (Load Pickup)	Breakers on bus 204 (BR 205, 206, 207) open.	Simultaneously open BR 205, 206, 207	Downstream loads picked up within 30 seconds.

Islanded mode and grid to island transition test scenarios

These test scenarios evaluate the controller's performance when the microgrid is operated in islanded mode and when the islanded MG reconnects to the utility grid. They demonstrate that (1) the DER-s of the microgrid can be controlled to support the seamless islanding of the MG when commanded (HIL.5); (2) the DER-s of the microgrid can be controlled to support the seamless islanding of the MG when no command is provided (HIL.6); (3) the DER-s of the microgrid can be controlled to support the connection of two adjacent islanded MGs (HIL.7).

Functionality	Simulated initiating event	Command from utility	Success criteria
HIL.5: Disconnect command (Planned Island)	POI relays at bus 101, 201, and 301 open after confirmation from MG	Disconnect command	Seamless transition from grid connected to islanded mode at prescribed time. V,f within allowable bands throughout.
HIL.6: Unplanned disconnect (Planned Island)	POI relays at bus 101, 201, and 301 open	N/A	Seamless transition from grid connected to islanded mode at prescribed time. V,f within allowable bands throughout.
HIL.7: Connect two adjacent microgrids (reconfiguration)	System operator	N/A	Seamless connection of two islanded MG. V,f within allowable bands throughout.
HIL.8: Loss of bus (Load pickup)	Breakers on bus 204 (BR 205, 206, 207) open.	Open BR 205, 206, 207	Downstream loads picked up within 30 seconds.

Island to grid transition test scenario

These test scenarios evaluate the controller's performance when the microgrid is an islanded MG reconnects to the utility grid. They demonstrate that (1) the DER-s of the microgrid can be controlled to support the seamless transition from islanded to grid connected mode within prescribed time (HIL.9).

Functionality	Simulated initiating event	Command from utility	Success criteria
HIL.9: Reconnect to the main grid	Utility signal that grid is operational	Grid Operational	Seamless transition from islanded to grid connected mode within prescribed time. V,f within allowable bands throughout.

Cyber-security test scenarios

These tests demonstrate that the controlled satisfies specific cyber-security requirements related to the confidentiality, integrity, and authenticity of the data, and that the controller remains functional even under DOS attacks.

Test/Concern	Attacker action	Expected behavior/Success criteria
CS.1: Confidentiality	Snoop on network packets	Attacker is unable to decode content
CS.2: Integrity	Modify and retransmit modified network packets	Modified packet is rejected by recipient
CS.3: Authenticity	Spoof network packets	Modified packet is rejected by recipient
CS.4: Availability	Flood network with packets	App detects the problem and acts accordingly

5.2 BASELINE CHARACTERIZATION

There were no predecessor implementations of a distributed microgrid controllers available, hence there was no baseline for the tests. In lieu of the baseline, the project has used the criteria specified by the IEEE as the baseline.

5.3 DESIGN AND LAYOUT OF TECHNOLOGY COMPONENTS

The overall architecture of the test setup is shown on Figure 17.

For testing purposes an extended Banshee microgrid model was used, the corresponds to the Banshee network model developed at the National Labs. The overall system topology and load profile has not been changed in the model that was be used in this technology demonstration. However, the generation mix has been updated to better reflect the scenario that IMCP is ideally suited for: a system with many smaller DERs that cooperate to maintain system stability. Table 5 summarizes the changes made to the Banshee network.

Table 5. List of Changes to the Banshee Model.

All batteries are 4-hour batteries.

Bus	Action	Change
103	Reduce capacity	Diesel Generator size from 4MVA to 2MVA
103	Addition PV	2MVA PV
104	Load change (C1)	Load capacity unchanged at 1200kVA; Changes: 200kVA shedable; BESS: 750kVA
106	Load change (C2)	Load capacity unchanged at 1500kVA; Changes: 500kVA shedable; BESS: 750kVA
202	Reduce capacity	Reduce ESS capacity from 2.5MVA 500kVA
204	Add Diesel	Add diesel with rating of 3.5MVA
209	Load change (C4)	Load capacity unchanged at 1000kVA; Changes: BESS: 750kVA
303	Load change (C5)	Load capacity unchanged at 1000kVA; Changes: BESS: 750kVA
306	Load change (C6)	Load capacity unchanged at 800kVA; Changes: BESS: 750kVA
306	Reduce capacity	CHP capacity from 3.5MVA to 2MVA; Generator changed from CHP to a Diesel Generator
307	Addition PV	2 MVA PV

The complete one-line diagram of the extended Banshee model is shown on Figure 19.

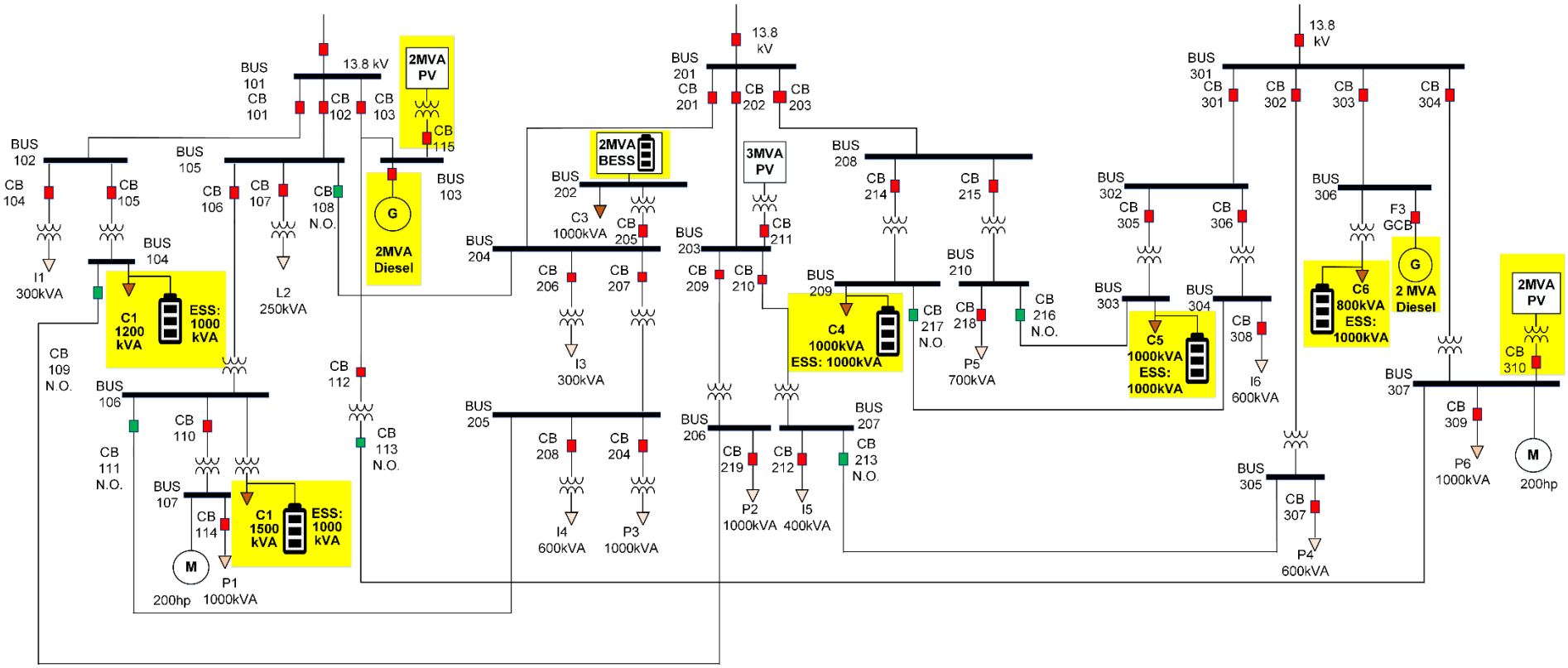

Figure 19. Microgrid Model Used in Testing

5.4 OPERATIONAL TESTING

The IMCP controller was tested at NCSU facility in the FREEDM lab using the facilities and the equipment described in Section 4 of this report.

The operational testing initially consisted of validating the Banshee MG implementation in OPAL-RT simulators. This consisted of validating the DER models in the simulation. In particular, care was taken to ensure that the DERs interfacing with hardware controllers are operating as expected. The validation consisted of sending MODBUS setpoints to a Texas Instruments F28377S microcontroller from the BBB and validating that these setpoints were correctly actuated in the OPAL-RT simulation.

Once the Banshee MG implementation in OPAL-RT was fully validated, this was followed by installing the IMCP controller on the testbed. This consisted of loading the distributed control algorithms on each node of the MG system. Different nodes were loaded with different sets of distributed algorithms, in accordance to the algorithms they are running. In particular relay nodes and the DER nodes are differentiated as described in Figure 9. The IMCP algorithm was instantiated for the Banshee network. Even though the underlying algorithms are generic, some level of customization is necessary due to the unique topology of each MG.

The IMCP was then tested in each operating mode of the MG individually to validate correct operation. The operating modes tested include the islanded operation and grid connected operation as well as the transitions functions. defined in Figure 2. Data for these preliminary tests was recorded using the OPAL-RT internal recording capabilities. As the simulation runs in real time, the simulator is able to capture data at numerous points at a pre-defined sampling rate. This data was then evaluated to ensure that all relevant data was captured without any errors. Following these preliminaries, the team executed the test plan HIL.1 through HIL.9, and the collected data is included in this report.

5.5 SAMPLING RESULTS

The project has developed: (1) the modified Banshee model that was simulated on an OPAL-RT high-fidelity real-time simulator, (2) the IMCP controller implementation code, (3) Modbus device interface components to connect to the (simulated) Banshee model, and (4) a graphical user interface for observing and controlling the IMCP.

The IMCP controller implements several ‘operating modes’ for grid-controlled, islanded, and transition operations. The transitions among these modes are orchestrated by a Finite State Machine, show on the figure.

All tests from the HIL and CS series have been successfully executed, and the results demonstrate the functionality of the IMCP.

The table below summarizes the tests and the demonstrated IMCP capabilities. The Appendix shows waveforms showing the test results.

Mode	Tests	Result – Demonstrated IMCP capability
Grid-connected	HIL1: Power Dispatch at POI	Dispatching real and reactive power from the microgrid DER-s proportionally to their ratings
	HIL2: Grid support at POI	Frequency/Watt mode dynamic reactive power support
	HIL 3: Power Factor Control at POI	Power factor control to support the main grid
	HIL 4: Loss of bus (load pickup)	Dispatching power to compensate for loss of bus
Islanding	HIL.5: Disconnect command (Planned Islanding)	Maintain control of the microgrid in case of planned islanding
	HIL.6: Unplanned disconnect (Unplanned Island)	Maintain control of the microgrid in case of unplanned, abrupt islanding
Islanded	HIL.7: Connect two adjacent microgrids (Reconfiguration)	Maintaining control while feeders are connected/disconnected
	HIL.8: Loss of bus (Load pickup)	Dispatching power to compensate for loss of bus
Islanded to grid-connected	HIL.9: Reconnect to the main grid	Facilitating seamless transition to grid-connected mode by controlling voltage/frequency/phase angel to achieve zero power transfer at POI.
Cybersecurity	CS.1: Confidentiality	Strong encryption of all network messages of application.
	CS.2: Integrity	Modified network messages are automatically rejected.
	CS.3: Authenticity	Network packets of invalid source are rejected.
	CS.4: Availability	Controller remains functional under network overload.

The cyber-security tests have been executed by monitoring the network packets (CS.1), monitoring the behavior of the application (CS.2 and C S.3), and observing the performance of the controller under adversary conditions (CS.4). The tests have verified that only encrypted messages were sent through the network (CS.1), that tampered and invalid messages were rejected before reaching the application code, and that the controller remained functional even if node became isolated due to a Denial-Of-Service (DOS) attack. As expected, the controller remained functional, although with lower performance, due to the lost messages. Once the attack ceased, the controller recovered.

6.0 PERFORMANCE ASSESSMENT

The project has implemented the test procedure on a HIL setup that allows for the monitoring of the system voltage and frequency throughout the test. The relevant voltage and frequency measurement were taken at all buses of the microgrids and the results show that the system met the performance requirements throughout the test. The key metric of interest was that the voltage and frequency of the system remained within the allowable IEEE 1547 range in all conditions.

Grid-connected mode test scenarios

Functionality tested	**Criteria met**
HIL.1: PQ dispatch	Value within 5% of rating within 30 seconds (IEEE 1547-2018 clauses 4.4)
HIL.2: Frequency Watt Mode; Dynamic Reactive Power Support	Value within 5% within 30 seconds (IEEE 1547-2018 clauses 4.4)
HIL.3: PF command	Value within 5% of rating within 30 seconds (IEEE 1547-2018 clauses 4.4)
HIL.4: Loss of bus (Load Pickup)	Downstream loads picked up within 30 seconds.

Islanded mode and grid to island transition test scenarios

Functionality tested	**Criteria met**
HIL.5: Disconnect command (Planned Island)	Seamless transition from grid connected to islanded mode at prescribed time. V,f within allowable bands throughout.
HIL.6: Unplanned disconnect (Planned Island)	Seamless transition from grid connected to islanded mode at prescribed time. V,f within allowable bands throughout.
HIL.7: Connect two adjacent microgrids (reconfiguration)	Seamless connection of two islanded MG. V,f within allowable bands throughout.
HIL.8: Loss of bus (Load pickup)	Downstream loads picked up within 30 seconds.

Island to grid transition test scenario

Functionality tested	**Criteria met**
HIL.9: Reconnect to the main grid	Seamless transition from islanded to grid connected mode within prescribed time. V,f within allowable bands throughout.

Cyber-security test scenarios

Concern tested	**Attacker action**	**Criteria met**
CS.1: Confidentiality	Snoop on network packets	Attacker is unable to decode content
CS.2: Integrity	Modify and retransmit modified network packets	Modified packet is rejected by recipient
CS.3: Authenticity	Spoof network packets	Modified packet is rejected by recipient
CS.4: Availability	Flood network with packets	Controller app detects the problem and acts accordingly

Note that the cyber-security tests were executed on an embedded system development board (BBB), configured with a stock Linux distribution (Ubuntu 20.04, for BBB). The board does not have an equipment certification (for example, FIPS PUB 140-2, CMMC 2.0, etc.

7.0 COST ASSESSMENT

7.1 COST MODEL

Considering that the testing and demonstration was executed in a university lab, cost estimates are not available. The table below summarizes the cost elements based on the team's understanding.

Cost Element	Explanation	Estimate
Software capital costs	Cost of software license for IMCP.	$0
	Cost of customization of IMCP software.	3-6 man-month
Hardware capital costs	Cost of embedded computers running IMCP	$0.5K/piece
	Cost of LAN to connect embedded computers.	~$20K
	Cost of custom hardware to connect IMCP to DERs	$0.5K/piece
Installation costs	Labor and material required to install	6 man-months
Maintenance	• Frequency of required maintenance	2-4 updates/year
	• Labor and material per maintenance action	1-3 man-month
Hardware lifetime	Estimate based on component obsolescence	5 years
Operator training	Training costs	0.5 man-month

7.1.1 Software costs

The developed technology: the IMCP and RIAPS software packages are made available under an open source license: Apache Version 2.0. The license can be summarized as follows (based on [1]):

"Under the Apache license, users are permitted to modify, distribute, and sublicense the original open source code. Commercial use, warranties, and patent claims are also allowed with the Apache license. The terms and conditions under the license don't place any restrictions on the code, but end users cannot hold the open source contributors liable for any reason.

When using the Apache license, developers must include the original copyright notice, a copy of the license text itself, and in some cases, a copy of the notice file with attribution notes and a disclosure of any significant changes made to the original code. Disclosing major code changes is a key differentiator between the Apache license and other permissive open source software licensing restrictions."

As such, commercial entities can freely use the software, as-is. However, there could be costs associated with (1) customizing the software for a specific microgrid installation, (2) extending to integrate non-Modbus based devices, and (3) developing a custom user interface.

[1] https://snyk.io/learn/apache-license/

7.1.2 Hardware capital costs

These costs are related to (1) the embedded computers IMCP runs on, (2) installing a LAN to connect the IMCP computers, and (3) adding custom hardware for interfacing specific DERs.

7.1.3 Installation costs

These costs include all material and labor costs for installing the IMCP system at a specific microgrid.

7.1.4 Maintenance

Following industry practice, the software needs to be updated 2-4 times per year, and each update may need 1-2 man/month of effort. Updates include defect fixes and security patches, including IMCP, RIAPS, and the supporting operating system: Linux.

7.1.5 Hardware lifetime

The typical lifetime of an embedded, industrial computer and/or network equipment is 5 years, possibly less. This is based on degradation due to exposure to ambient conditions and the hardware obsolescence.

7.1.6 Operator training

While IMCP runs on embedded computers, operators need to be trained to (1) install updates of IMCP on the system, and (2) possibly interact with IMCP to initiate specific control actions (e.g. connecting/disconnecting to/from the utility grid).

7.2 COST DRIVERS

Cost drivers include:

- Software engineering costs to customize IMCP, to add new DER interfaces to IMCP, and to customize the user interface.
- Hardware costs for embedded computers and LAN equipment
- Labor and material costs for installing the IMCP
- Costs of operating: maintaining the computers with software updates, controlling IMCP manually (if needed), maintain the network equipment, including power supplies, etc.

7.3 COST ANALYSIS

The IMCP software is universally applicable to microgrids. In its current, demonstrated form, it can be used with DERs that implement the Modbus/TCP protocol and are able to supply sensor data for the IMCP application and to receive setpoint commands from it.

IMCP is available under an open source license. Hence, the total life-cycle cost of an IMCP installation depends on the engineering, material, and labor costs of that specific installation, with the baseline IMCP cost being zero.

Current microgrid controllers are centralized: they rely on a single, possibly expensive central controller, with custom wiring connecting it to the individual DERs of the microgrid. IMCP, in contrast, relies on a field-quality LAN connecting small, low-cost, industrial embedded computers directly attached to the DERs, with direct wiring.

Given the commercial availability of low-cost industrial embedded computers and LAN equipment, and given that open source license for the software, arguably, IMCP is a cost-effective solution to implement microgrid controllers.

8.0 IMPLEMENTATION ISSUES

The development project has not encountered any significant implementation issues. The implementation and its testing were performed in a laboratory environment, using simulated power systems. The simulator was a high-performance, high-fidelity, real-time simulator (OPAL-RT), that also implemented the real-time hardware/software interfaces (specifically: the Modbus protocol) that is expected in a field environment. The IMCP software was running on a network of Beaglebone Black devices: small form factor, embedded computing devices, connected to an isolated LAN in the lab.

However, for fielding the results of the project, i.e., the control algorithm implementations state-of-the-art embedded, industrial-grade computing devices are needed, that have (1) local area network interfaces with support for IEEE 1588 - Precision Time Protocol (PTP), and (2) interfaces to local DER-s (e.g. Modbus of serial ports). The industrial embedded computers need to be housed in field-grade enclosures, must have uninterruptible power supplies (UPS), and need to connect to a local area network.

The interfaces to the power devices (DERs) need to be designed according to the requirements of the field environment. IMCP and RIAPS were designed to be integrated easily with existing DERs. The IMCP demonstration has used the Modbus protocol, and the RIAPS packages include support for other protocols, including IEEE 37, MQTT, and CAN bus. Additional protocols are feasible, but their implementation needs to be developed. In all cases, the protocol implementation in a generic software component has the augmented with configuring the interface for the specific MG DER's address and other parameters.

The developed software code base: the microgrid controller and the software platform is open source, and as such can be used by developers of microgrids. However, it is necessary to customize it to a specific microgrid configuration and power system devices.

9.0 RESULTS AND DISCUSSION

The above results show that the proposed distributed generic MG controller can support grid-connected operation, planned/unplanned islanding, islanded operation, and reconnecting of MGs, as well as can address cyber-security concerns. Throughout the tests, the proportional active and reactive power sharing among DERs was maintained. Smooth transitions between states were achieved.

For fielding the controller, more development work is necessary, as listed below.

- **Hardware platform**. Due to supply chain issues (COVID-19), industrial-quality embedded computing hardware was not obtained. However, several options are available, including, for example, IoT gateways and similar edge computing devices. Given experience with the BBB and other, experimental embedded computing devices (e.g. Raspberry Pi), no difficulties are anticipated.
- **Fault management**. For field deployment, safe operation is essential, even if some parts of the system (e.g. computing nodes, network connections, or low-level controllers) fail. The RIAPS platform provides basic functions for implementing fault-tolerant systems, but in itself does not solve the problem. While testing showed the robustness of the platform in a lab environment, the controller algorithms have to be tested under filed conditions and potentially revised such that the resulting microgrid control system is fault tolerant.
- **Integration with other systems**. IMCP is a Level 2 microgrid controller, but, in a field environment, it needs to communicate with other systems (e.g. energy or building management systems, or inverters, protection systems, etc.). RIAPS provides the basic technology to implement such interfaces, but they need to be developed for specific microgrids and hardware. See discussion in previous sections.

10.0 IMPLICATIONS FOR FUTURE RESEARCH AND BENEFITS

Building on the RIAPS platform's capabilities, the project has developed a framework for implementing distributed generic MG controllers. In the distributed control paradigm, each MG asset (e.g., a relay or a DER) has an associated computational node (e.g., a single board computer with a network interface) that is equipped with communication and computation capability. The MG assets are coordinated by distributed algorithms on the computational nodes to achieve the desired control goals. By abstracting the roles of the assets, distributed algorithms are designed to be consistent for each type of MG assets regardless of their underlying properties. Therefore, it is re-usable in different scenarios and naturally supports plug-and-play capability. Furthermore, the distributed nature of the architecture allows the control and coordination of networked microgrids – a novel architecture. Distributed control provides a viable solution to many of the challenges faced by centralized control such as scalability, modularity and resilience.

The project demonstrated the microgrid controller framework on the Banshee network, a complex nested microgrid, with multiple topologies. The demonstration has shown the capacity to form and break up microgrids following an operator command. In the process, it was established that the collection of distributed algorithms effectively covers all of the microgrid operational use cases and that the end product effectively delivers a cyber secure solution.

The IMCP framework provides a solution for the Level 2 control problems in microgrids, but several related research questions remain, including but not limited to: optimal operation of breakers in a microgrid in case of faults, completely automated blackstart functionality, and the overall microgrid design problem with respect to equipment sizing and location to achieve optimal (cost effective and robust) performance.

While the completed project significantly de-risks the technology, additional steps are needed before a field implementation. First, a field-ready, industrial quality single-board computer are needed that can run the RIAPS and IMCP codes. The demonstrations were using the Beaglebone Black single board computer. Second, even though the HIL environment provides a high level of fidelity, and allows for testing of complex use cases at edge conditions, there is a need for a "field implementation" to demonstrate that the platform can work with off-the-shelf DERs. In other words, a field demonstration of the technology on a physical microgrid is needed.

For a DoD field implementation – or any other microgrid installation, a commercial vendor is to provide the actual electrical engineering design, equipment selection, and physical installation work. The IMCP code base can be used and configured by qualified software engineers for the needs of the specific microgrid. In an earlier section of this report cost estimates are provided for these activities. As discussed earlier, the IMCP source code is available under an open source license, but it needs to be customized and possibly extended for specific microgrid equipment. However, savings are expected in terms of software development costs, as the core algorithms and the platform has been extensively tested in the course of the project and highly reusable.

11.0 REFERENCES

[1] "Metrics and Standards for Energy Resilience at Military Installations ", available from https://www.acq.osd.mil/eie/Downloads/IE/Metrics%20and%20Standards%20for%20Energy%20Resilience%2020%20May%202021.pdf

[2] Salcedo, Reynaldo, Edward Corbett, Christopher Smith, Erik Limpaecher, Raajiv Rekha, John Nowocin, Georg Lauss et al. "Banshee distribution network benchmark and prototyping platform for hardware-in-the-loop integration of microgrid and device controllers." The Journal of Engineering 2019, no. 8 (2019): 5365-5373.

[3] Eisele, Scott, Istvan Madari, Abhishek Dubey, and Gabor Karsai. "RIAPS: Resilient information architecture platform for decentralized smart systems." In 2017 IEEE 20th International Symposium on Real-Time Distributed Computing (ISORC), pp. 125-132. IEEE, 2017.

[4] Z. Zhang and M. Chow, "Convergence analysis of the incremental cost consensus algorithm under different communication network topologies in a smart grid," IEEE Transactions on Power Systems, vol. 27, no. 4, pp. 1761–1768, 2012.

[5] H. Tu, Y. Du, H. Yu, S. Meena, X. Lu, and S. Lukic, "Distributed economic dispatch for microgrids tracking ramp power commands," IEEE Transactions on Smart Grid, vol. 14, no. 1, pp. 94–111, 2023.

[6] J. W. Simpson-Porco, Q. Shafiee, F. Dorfler, J. C. Vasquez, J. M. Guerrero, and F. Bullo, "Secondary frequency and voltage control of islanded microgrids via distributed averaging," IEEE Transactions on Industrial Electronics, vol. 62, no. 11, pp. 7025–7038, 2015.

[7] Y. Du, H. Tu, and S. Lukic, "Distributed control strategy to achieve synchronized operation of an islanded microgrid," IEEE Transactions on Smart Grid, vol. 10, no. 4, pp. 4487–4496, 2019.

APPENDIX A POINTS OF CONTACT

Point of Contact Name	Organization Name Address	Phone Fax Email	Role in Project
Gabor Karsai	Vanderbilt University 1025 16th Avenue South Nashville, TN 37212	615 343 7471, 615 343 7440, gabor.karsai@vanderbilt.edu	PI
Srdjan Lukic	North Carolina State University, 1791 Varsity Drive, St100, Raleigh, NC 27606	312 925 5031, N/A smlukic@ncsu.edu	Co-PI

APPENDIX B SUPPORTING DATA

Listed below are the summaries of HIL tests, together with charts showing the controller's performance over time.

HIL1: POWER DISPATCH AT POI – FEEDER 1

The goal of this test was to show that the IMCP platform can follow a power dispatch command. This test was performed on Feeder 1 of the Banshee MG with the MG connected to the utility. The active power dispatch was determined based on a quadratic cost curve, which is set at $C_{dg1} = C_{dg2} = 0.025P^2 + 8P$ for the Diesel Generator (GEN) and at $C_{gen} = 0.005P^2 + 20P$ the BESS. The POI power command was initially set at zero. At two minutes, the power command was changed to $P = 800kW;\ Q = 0kVAR$, whch corresponds to a larger power inport from the grid. As a result, the power from the DERs within the MG is reduced. Power is shared according to the quadratic relationships defined earlier. The system reaches a steady state within a few seconds. Four minutes into the simulator, the power command is changed to $P = 800kW;\ Q = 600kVAR$. Since the reactive power is shared proportionally, in steady state all of the reactive power commands overlap. Additional operating points are considered 6 minutes into the simulation ($P = 400kW;\ Q = 600kVAR$) and 8 minutes into the simulation ($P = 400k\ ;\ Q = 300kVAR$). The performance is as expected with proportional reactive power sharing and real power sharing following the DER's cost curves.

Test Summary:

- POI power is controlled to follow the reference
- Active power is shared among DERs according to cost curve:
  - $C_{dg1} = C_{dg2} = 0.025P^2 + 8P$
  - $C_{gen} = 0.005P^2 + 20P$
- Reactive power is shared proportionally to the ratings
  - $S_{dg1} = S_{dg2} = 1\ MVA$
  - $S_{gen1} = 2\ MVA$
- PV output is high
  - $S_{pv1} = 2\ MVA$

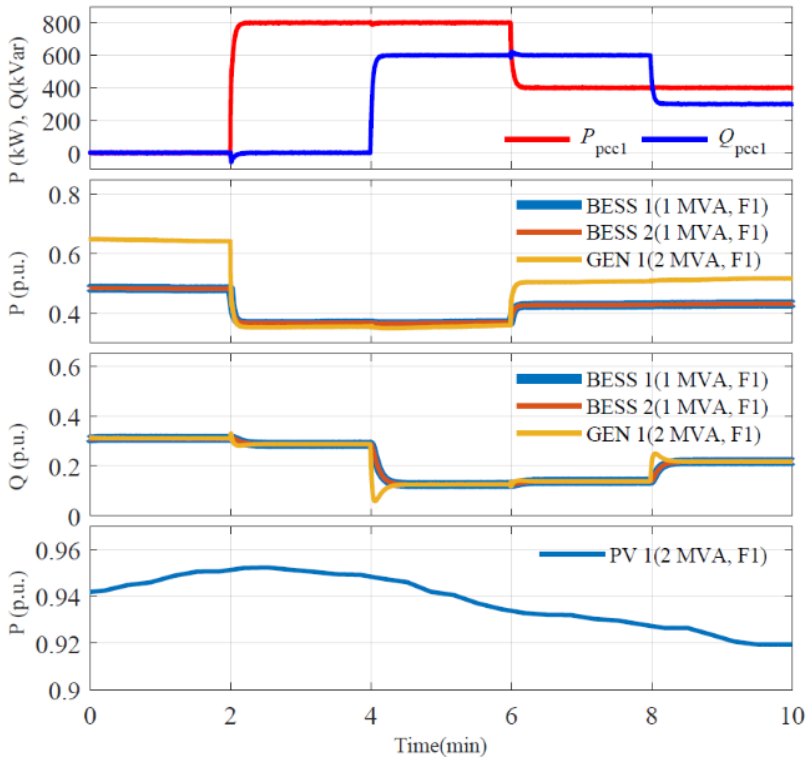

HIL2: GRID SUPPORT AT POI- FEEDER 1

The goal of this test was to show that the IMCP platform can follow a droop characteristic. This test was performed on Feeder 1 of the Banshee MG with the MG connected to the utility. The active power dispatch was determined based on a quadratic cost curve, which is set at $C_{dg1} = C_{dg2} = 0.025P^2 + 8P$ for the Diesel Generator (GEN) and at $C_{gen} = 0.005P^2 + 20P$ the BESS. Two minutes into the simulation, the frequency of the grid is ramped down from 60Hz to 59.5Hz. As a result, the power output from the generators is increased in accordance to the droop characteristics. As the frequency is then ramped up to 60.5Hz the real power output from the DERs reduces accordingly following the P-f droop characteristic. The reactive power command remains unaffected by the frequency variation. 4 minutes into the simulation, the POI voltage is varied from 1pu down to 0.95pu and then back up to 1.05 pu. The reactive power output from the DERs varies according to the Q-V droop characteristic.

Test Summary:

- Measured f and V at POI, vary as designed
- POI active power and reactive power follow the f and V
- Active power is shared among DERs according to cost curve:
  - $C_{dg1} = C_{dg2} = 0.025P^2 + 8P$
  - $C_{gen} = 0.005P^2 + 20P$
- Reactive power is shared proportionally to the ratings
  - $S_{dg1} = S_{dg2} = 1\ MVA$
  - $S_{gen1} = 2\ MVA$
- PV output is high
  - $S_{pv1} = 2\ MVA$

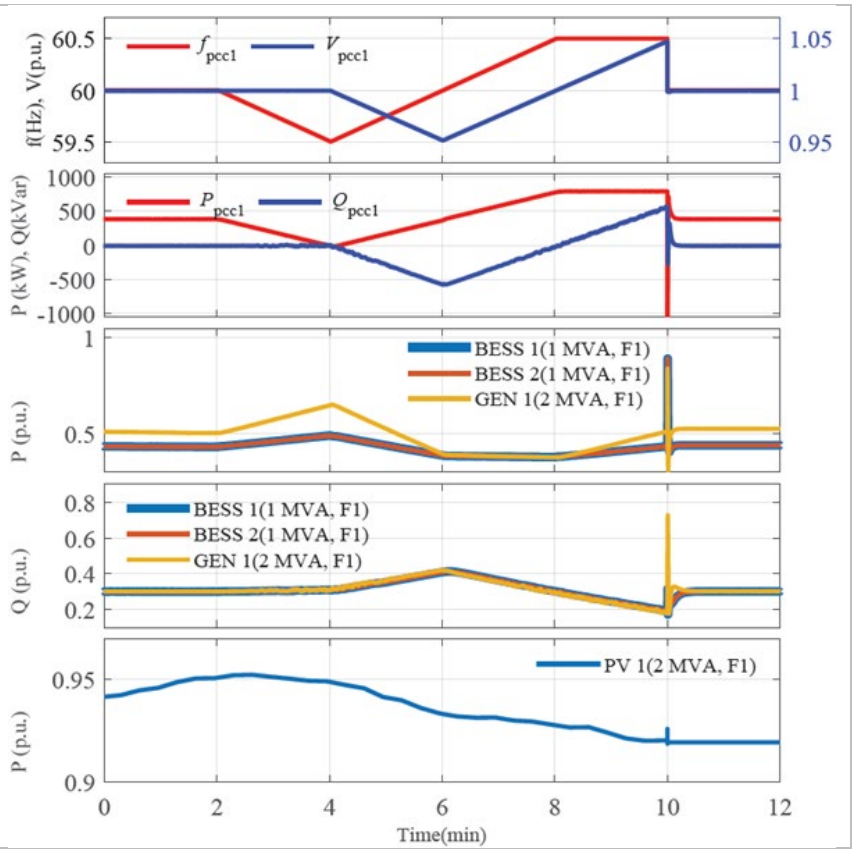

HIL 3: POWER FACTOR CONTROL AT POI

The goal of this test was to show that the IMCP platform can follow a dynamic power factor dispatch command. This test was performed on Feeder 1 of the Banshee MG with the MG connected to the utility. The active power dispatch was determined based on a quadratic cost curve, which is set at $C_{dg1} = C_{dg2} = 0.025P^2 + 8P$ for the Diesel Generator (GEN) and at $C_{gen} = 0.005P^2 + 20P$ the BESS. The POI real power command slowly ramps up from to $P = 400kW$, then to $P = 800kW$, and back down to $P = 400kW$, reaching a peak at 4 minutes. The power factor command was held steady at 0.75PF lagging. At 4 minutes, the power factor command

ramps up from 0.75pf lagging to 0.95 PF lagging. The reactive power is shared proportionally among the DER-s and the reactive power injection curves overlap over the entirety of the test. At 4 minutes, when the power factor command changes from 0.75PF lagging to 0.95 PF lagging the reactive power injection reduces accordingly.

Test Summary:

- POI active power and PF follow the command
- Active power is shared according to cost curve:
  - $C_{dg1} = C_{dg2} = 0.025P^2 + 8P$
  - $C_{gen} = 0.005P^2 + 20P$
- Reactive power is shared proportionally to the ratings
  - $S_{dg1} = S_{dg2} = 1\ MVA$
  - $S_{gen1} = 2\ MVA$
- PV output is high
  - $S_{pv1} = 2\ MVA$

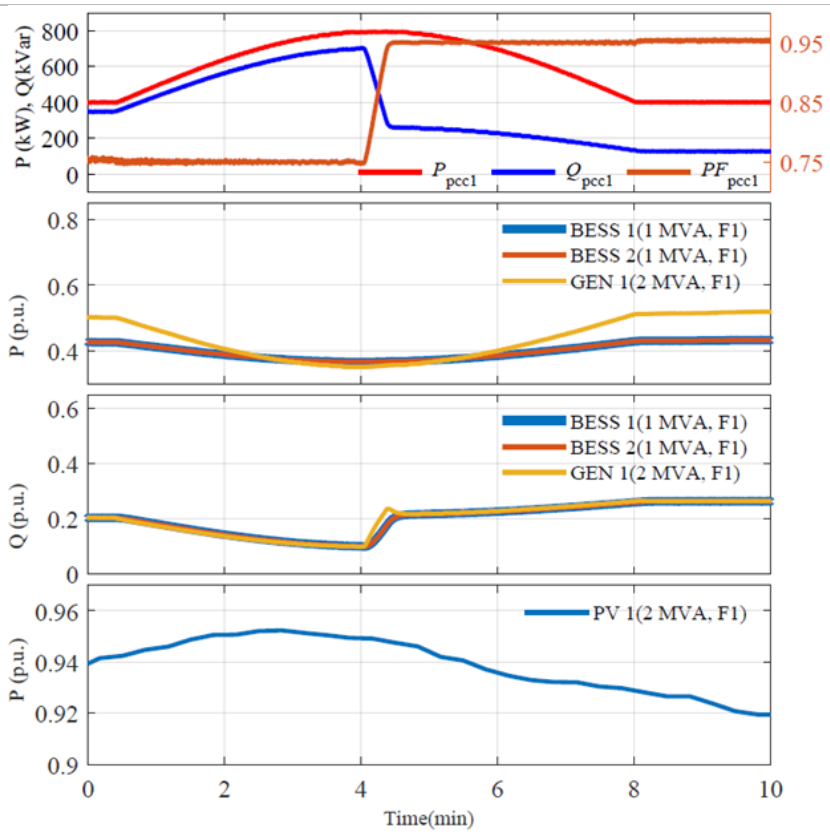

HIL 4: Loss of bus in grid-connected mode

The goal of this test was to show that the IMCP platform can successfully transfer a load from one feeder to another. This may be necessary to reduce demand on a given feeder, or to back feed a load after a fault occurs upstream on a feeder. In this case, Bus 205, which is powered by Feeder 2, is disconnected from feeder 2 and reconnected to Feeder 1. Initially, all the feeders are connected to the grid. All the normally-open breakers are open and the system is operating at steady state. Five seconds into the simulation, breaker 207 opens and bus 205 is deenergized. Due to the reduction in load on Feeder 2, the real and reactive power flow at the POI of feeder 2 reduces at 2 seconds. At 12 seconds since the start of the simulation, breaker 111 closes and connects the load connected to bus 205 into feeder 1. This is reflected by an increase in the power at the POI of feeder 1. In this test Feeder 3 is unaffected as shown in the plot below.

Test Summary:

- Initially, all the feeders are connected to the grid. All the normally-open breakers are open
- Breaker 207 opens at t=5 s
- Bus 205 will be de-energized
- Closing ON breaker 111 will re-energize bus 205 again

Feeder 2: 207 opens

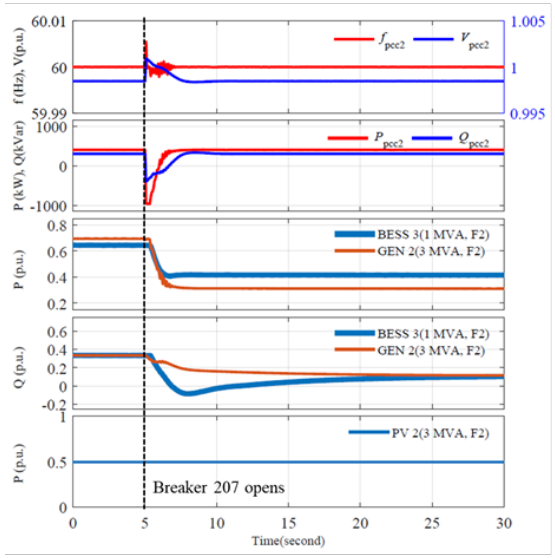

Feeder 1: 111 closes

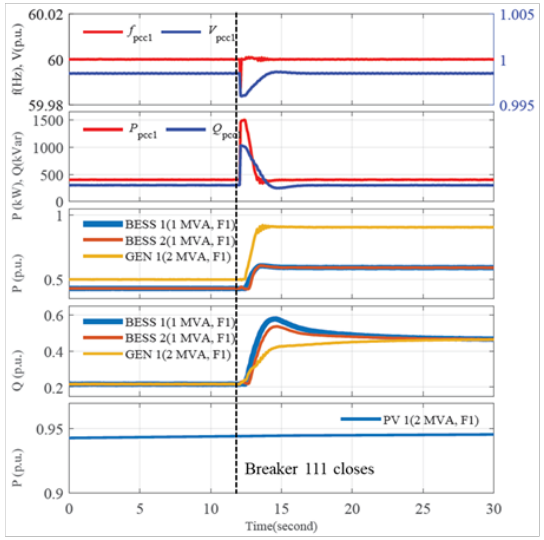

Feeder 3:

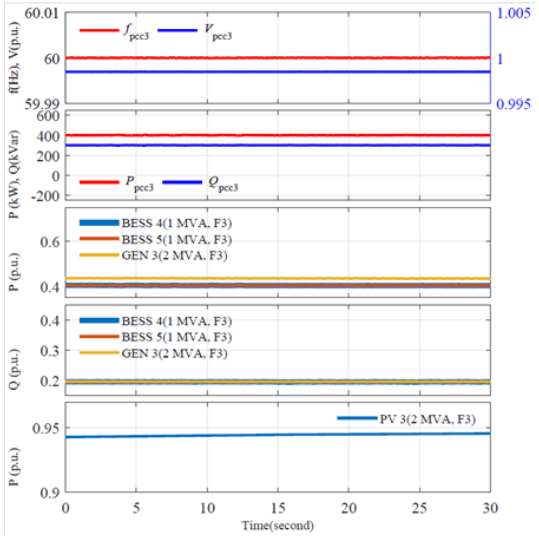

HIL 5: PLANNED ISLANDING – FEEDER 1

The goal of this test was to show that the IMCP platform can successfully prepare a feeder for an intentional islanding event. Before islanding, POI active power and reactive power follow the reference $P_{POI} = 400\ kW$ and $Q_{POI} = 300\ kVar$. The active power is shared according to cost curve $C_{dg1} = C_{dg2} = 0.025P^2 + 8P$ and $C_{gen} = 0.005P^2 + 20P$ while the reactive power is shared proportionately. At 10 seconds into the simulation, the "prepare for islanding" command is received. As a result, the POI active power and reactive power are regulated to 0. This process completes at about 14 seconds (in about 4 seconds) and the POI relay automatically disconnects when it senses that the power flow is below a threshold. The system then operates in islanded mode from 14 seconds onwards.

Test Summary:

- Measured f and V at microgrid POI
- Before islanding, POI active power and reactive power follow the reference $P_{POI} = 400\ kW$ and $Q_{POI} = 300\ kVar$.
- During islanding, POI active power and reactive power are regulated to 0.
- Before islanding, active power is shared according to cost curve:
  - $C_{dg1} = C_{dg2} = 0.025P^2 + 8P$
  - $C_{gen} = 0.005P^2 + 20P$
- During/after islanding active power is shared proportionally to the ratings
- Reactive power is shared proportionally to the ratings
  - $S_{dg1} = S_{dg2} = 1\ MVA$
  - $S_{gen1} = 2\ MVA$
- PV output is high
  - $S_{pv1} = 2\ MVA$

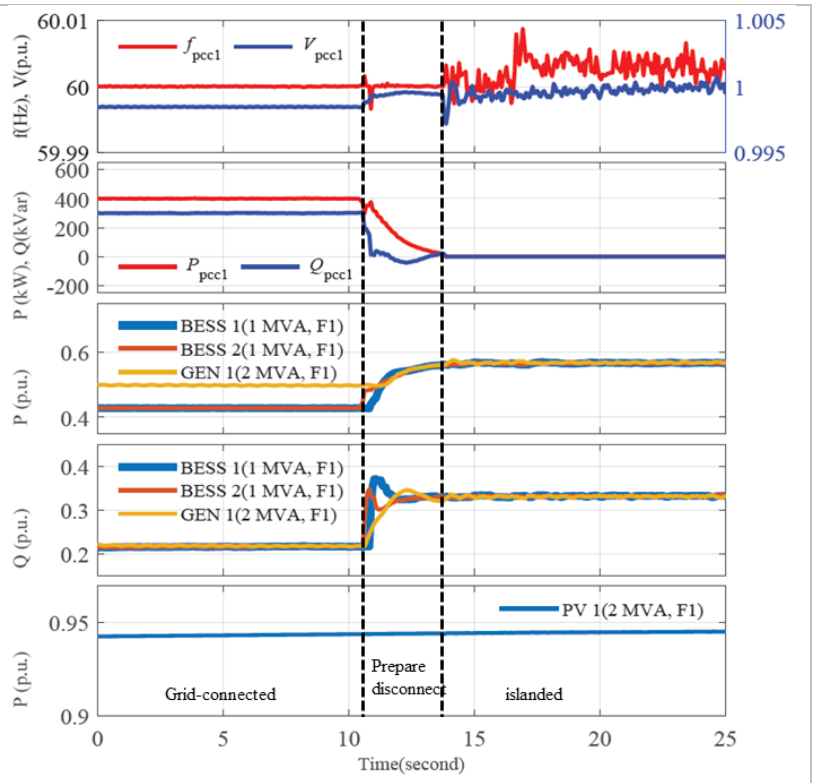

HIL 6: UNPLANNED ISLANDING - FEEDER 1

The goal of this test was to show that the IMCP platform can successfully handle an unplanned islanding event. In this test the POI breaker opens with no forewarning when the simulation time is 10 seconds. Before islanding, POI active power and reactive power follow the reference $P_{POI} = 400\,kW$ and $Q_{POI} = 300\,kVar$. The active power is shared according to cost curve $C_{dg1} = C_{dg2} = 0.025P^2 + 8P$ and $C_{gen} = 0.005P^2 + 20P$ while the reactive power is shared proportionately. At 10 seconds into the simulation, the POI breaker opens. After islanding active and reactive power are shared proportionally. The system successfully islands and voltage and frequency are regulated at nominal values in islanded operating mode.

Test Summary:

- Measured frequency and voltage at microgrid POI
- Before islanding, POI active power and reactive power follow the reference
  - $P^*_{POI} = 400\,kW$
  - $Q^*_{POI} = 300\,kVar$
- Before islanding, active power is shared according to a cost curve
- After islanding active and reactive power are shared proportionally
- Reactive power is shared proportionally to the ratings
  - $BESS\ 1{,}2\ = 1\,MVA$
  - $Generator\ 1\ = 2\,MVA$

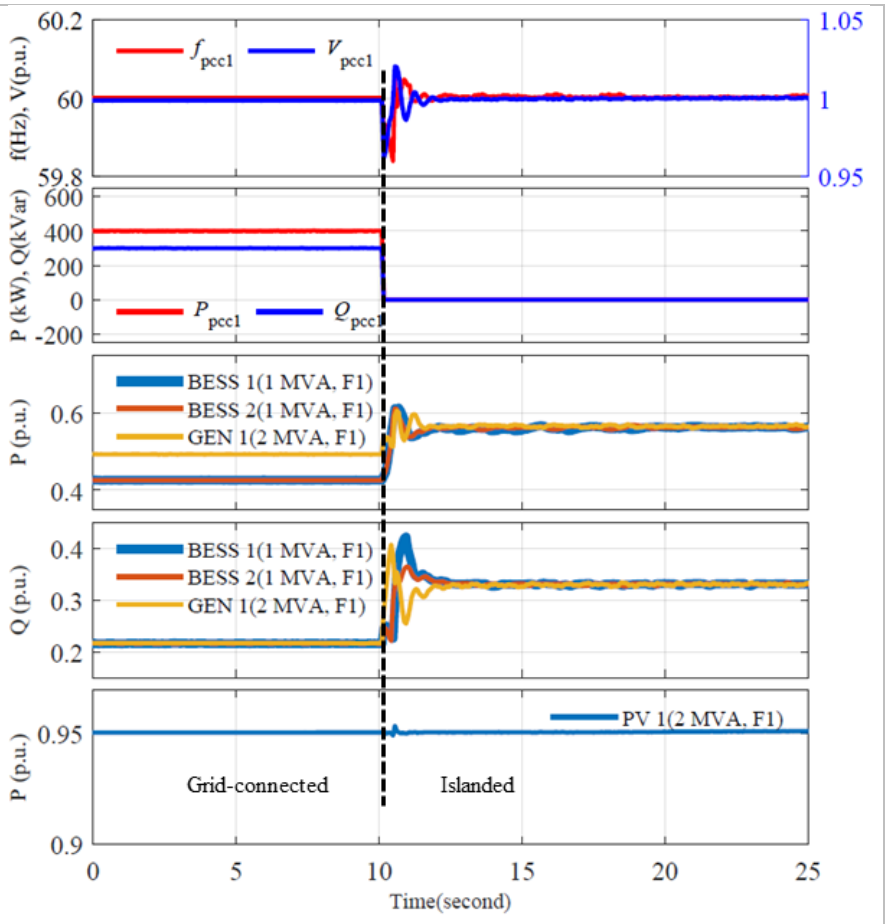

HIL 7: DISCONNECT TWO ADJACENT MICROGRIDS (RECONFIGURATION)

The goal of this test was to show that the IMCP platform can successfully break a large MG into smaller MG-s. The reverse process was also tested (connect two adjacent microgrids) and it is presented in HIL 10. In this test, initially the Banshee network is operating in islanded mode, with the entire Banshee network operating as a single microgrid made up of feeders 1-3. 10 seconds into the simulation, a command is given to separate Feeder 3 MG from combined MG made up of

feeders 1 and 2. The real power command is brought to zero within two seconds, while the reactive power flow takes longer to bring down to zero (about 20 seconds). This is due to the low action of the integrator in the reactive power control loop. At 30 seconds feeder 3 is disconnected from the combined MG made up of feeders 1 and 2. 60 seconds into the simulation a command is given to disconnect feeder 1 MG from Feeder 2 MG. The power flow between the two MG is brought to zero within two seconds, and the system is ready for disconnection. The command for the tie-line relay to open is given 70 seconds into the simulation, bringing the test to a successful conclusion.

The events of the scenario are described under the chart.

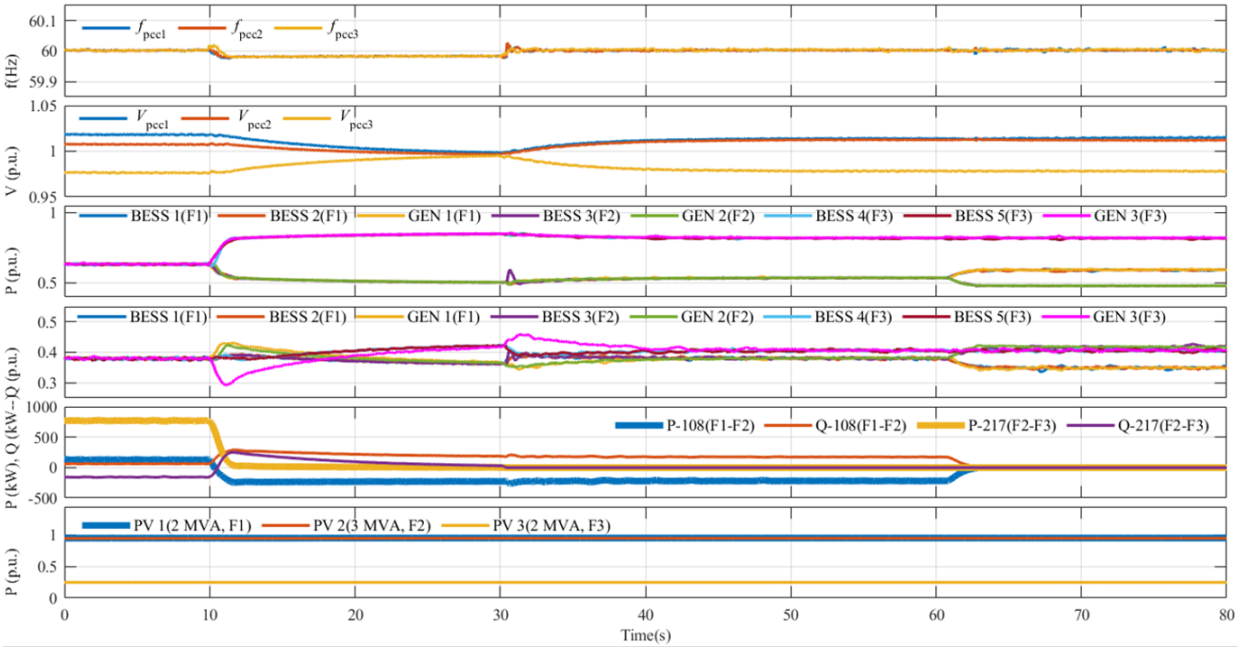

F1F2F3 Islanded | Disconnecting F1F2-F3 | F1F2 Islanded F3 Islanded | Disconnecting F1-F2 | F1 Islanded F2 Islanded F3 Islanded

HIL 8: LOSS OF BUS (LOAD PICKUP) IN ISLANDED MODE

The goal of this test was to show that the IMCP platform can move a load from one MG to another adjacent microgrid. Initially, all the feeders are disconnected from the grid. All the normally open breakers are open. Five seconds into the test, Breaker 207 opens and Bus 205 becomes de-energized. At 15 seconds, the Breaker 111 is turned ON and will re-energize bus 205 again, making bus 205 now a part of Feeder 1 MG. This represents a load pickup in islanded mode. At 5 seconds, when load on Bus 205 was disconnected from Feeder 2 MG, the voltage transient has a peak to 1.09 p.u.; frequency transient has a peak to 60.14 Hz (complied with IEEE 1547 settings selected). At 15 seconds, when load on Bus 205 was connected to Feeder 1 MG, the voltage transient has a peak to 0.92 p.u.; frequency transient has a peak to 59.78 Hz (complied with IEEE 1547 settings selected). Feeder 3MG is not a part of this reconfiguration test, and its voltage and frequency show no significant deviation throughout the test. Throughout the test the active and reactive power is shared proportionally to the DER ratings.

Test Summary (feeder 2)

- Voltage transient has a peak to 1.09 p.u.; frequency transient has a peak to 60.14 Hz
- POI active power and reactive power are zero
- Active and reactive power shared proportionally to the ratings

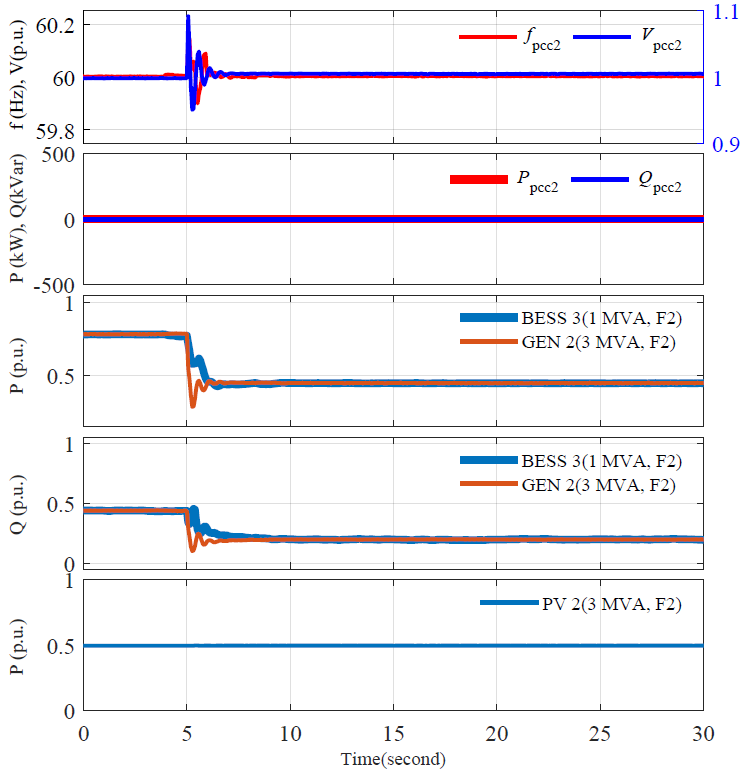

Test Summary (feeder 1)

- Voltage transient has a peak to 0.92 p.u.; frequency transient has a peak to 59.78 Hz.
- POI active power and reactive power are zero
- Active and reactive power shared proportionally to the ratings

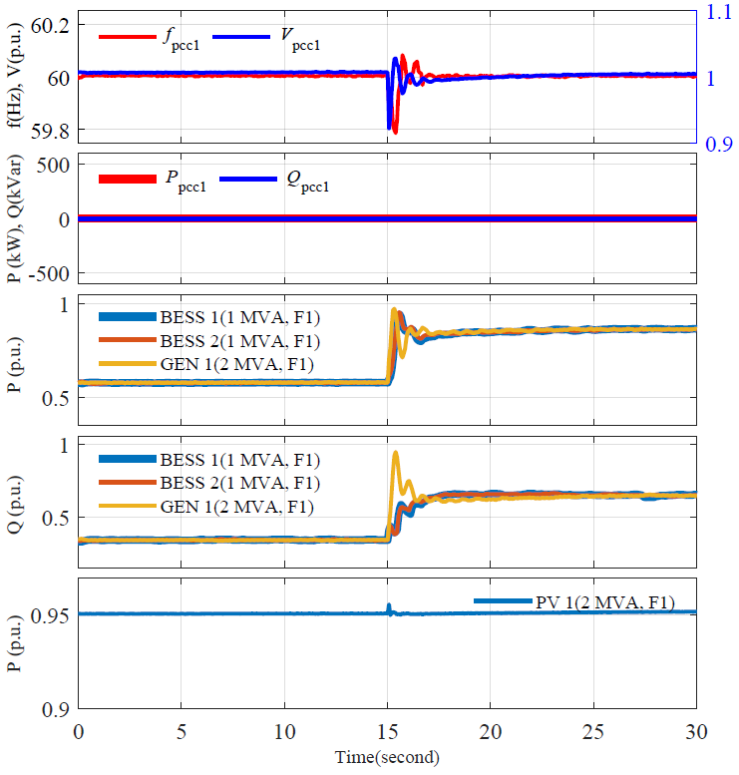

Test Summary (feeder 3)

- Frequency and voltage are regulated to rated values
- POI active power and reactive power are zero
- Active and reactive power shared proportionally to the ratings

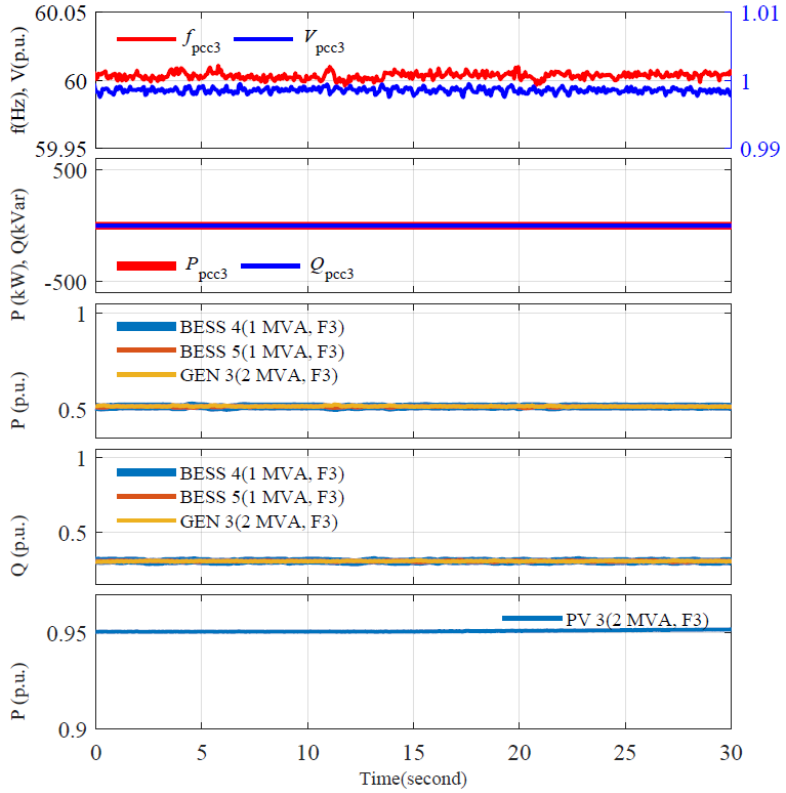

HIL 9: RECONNECTING TO THE GRID – FEEDER 1

The goal of this test was to show that the IMCP platform can reconnect a MG to the utility grid. This is achieved by bringing the phasors of the voltage at either side of the opened POI relay to be synchronized. Using the resynchronization algorithm described earlier, the power commands at each DER are adjusted to slowly eliminate the voltage magnitude and phase errors between the two measurements. In this test, the resynchronization process is initiated 5 seconds into the test and completed at 10 seconds when the POI relay automatically closes. Before reconnecting active power is shared proportionally to the ratings of the DERs, while after reconnecting, active power is shared according to cost curve$C_{dg1} = C_{dg2} = 0.025P^2 + 8P$ and $C_{gen} = 0.005P^2 + 20P$.

Test Summary:

- Measured frequency and voltage at microgrid POI
- After reconnecting, POI active power and reactive power follow the reference
  - $P_{POI} = 400\ kW\ and$
  - $Q_{POI} = 300\ kVar.$
- Before reconnecting active power is shared proportionally to the ratings
- After reconnecting, active power is shared according to cost curve:
  - $C_{dg1} = C_{dg2} = 0.025P^2 + 8P$
  - $C_{gen} = 0.005P^2 + 20P$
- Reactive power is shared proportionally to the ratings
  - $S_{dg1} = S_{dg2} = 1\ MVA$
  - $S_{gen1} = 2\ MVA$
- PV output is high
  - $S_{pv1} = 2\ MVA$

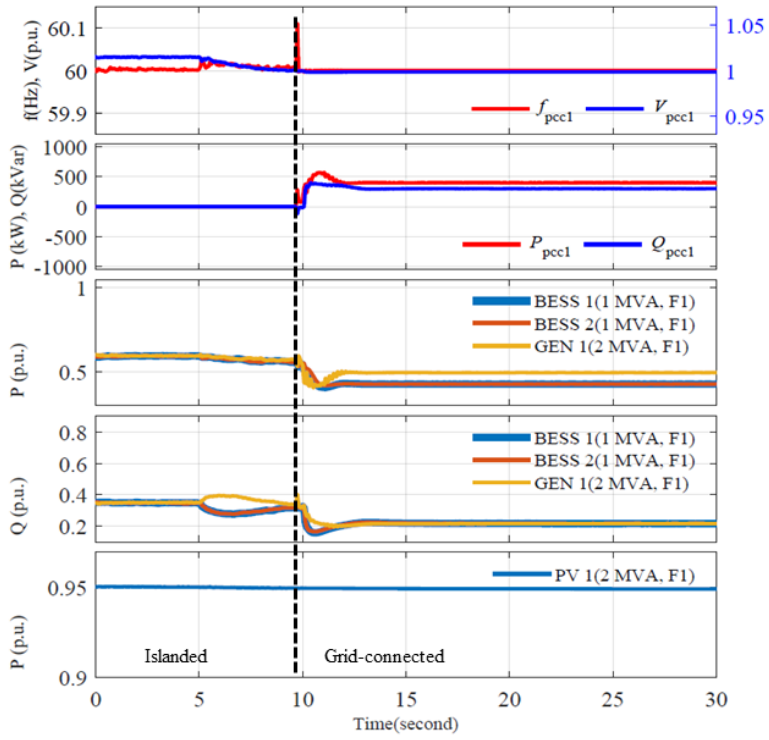

HIL 10: COMPREHENSIVE TEST

This test was added late in the project, and it exercises all the functions of the controller. The events of the test are summarized below the figure. The test begins with the MG operational but without the IMCP controller active. At 10 seconds into the simulation, the controller is enabled and the, active power is shared according to cost curve$C_{dg1} = C_{dg2} = 0.025P^2 + 8P$ and $C_{gen} = 0.005P^2 + 20P$ While the reactive power is shared proportionally. 30 seconds into the simulation the system is islanded, with the three feeders making up three separate MG-s. A command to connect feeders 1 and 2 into a larger MG is given at 75 seconds, a process that completes in about 5 seconds. A command to connect feeder three to the MG made up of feeder 1 and 2 is given 100 seconds into the simulation, a process that takes about 5 seconds. The system now operates as a large islanded microgrid. Throughout the island operation, both real and reactive power are shared proportionally. This is visible in the per-unit real and reactive power plot in the time period between 100 and 140 seconds, where all generator outputs overlap. 140 seconds into the simulation a command is given to separate feeder 3 into a separate MG. This process is completed after about 5 seconds. 180 seconds into the simulation a command is given to separate feeder 1 MG from Feeder 2 MG. This process is also completed in less than 5 seconds. Around 200 seconds into the simulation, the three MG are all islanded and operating independently. 230 seconds into the test a command is given to reconnect the three MG to their respective POI's. The three MG are grid connected again 20 seconds into the simulation.

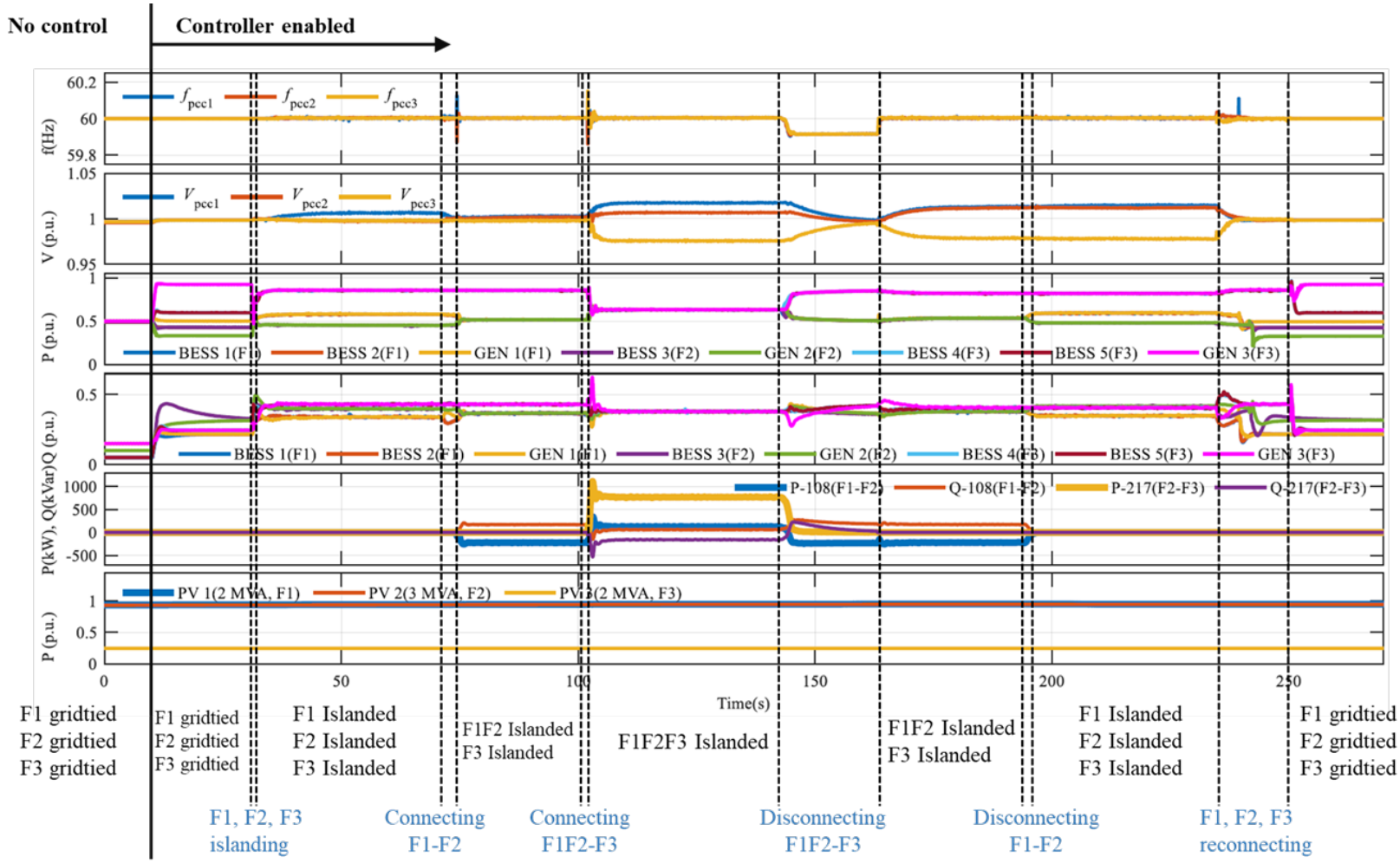
No control
Controller enabled
f(Hz)
V (p.u.)
P (p.u.)
Q(kVar) (p.u.)
P(kW), Q(kVar)
P (p.u.)
Time(s)
F1 gridtied
F2 gridtied
F3 gridtied
F1 gridtied
F2 gridtied
F3 gridtied
F1 Islanded
F2 Islanded
F3 Islanded
F1F2 Islanded
F3 Islanded
F1F2F3 Islanded
F1F2 Islanded
F3 Islanded
F1 Islanded
F2 Islanded
F3 Islanded
F1 gridtied
F2 gridtied
F3 gridtied
F1, F2, F3 islanding
Connecting F1-F2
Connecting F1F2-F3
Disconnecting F1F2-F3
Disconnecting F1-F2
F1, F2, F3 reconnecting

APPENDIX C END-USER AND PROCUREMENT PRODUCTS SUPPORTING DAT

As discussed in the report the project resulted in two major software packages: one for the distributed software platform, and one for the actual microgrid controller. For the second, the project has built additional software packages that interface the microgrid controller software to human operators, as well as power system devices (e.g. inverters, relays, etc.). The products are published on Github, in the form of open-source repositories, with additional documentation and demonstration materials linked to in the content. The repositories are listed below, together with their short descriptions.

RIAPS PLATFORM REPOSITORIES

These repositories contain the source code and documentation for the RIAPS software platform.

- riaps-pycom https://github.com/RIAPS/riaps-pycom The main repository of the RIAPS code base. It contains all the Python implementation code for the RIAPS platform.
- https://riaps-pycom.readthedocs.io/en/latest/ Documentation site for the RIAPS platform.
- riaps-timesync https://github.com/RIAPS/riaps-timesync Repository for the time-synchronization service. Uses the IEEE 1588 Precision Time Protocol to synchronize the clocks of the RIAPS nodes.
- riaps-integration https://github.com/RIAPS/riaps-integration Repository for all scripts to build release packages for RIAPS.

In the course of the IMCP project, the RIAPS platform has been significantly updated to meet the needs of the IMCP control application.

IMCP PLATFORM REPOSITORY

This repository contains the code base and documentation for the Integrated Microgrid Control Platform. Note that the IMCP code in this repository was created to control the extended 3-feeder Banshee model, as configured to run an OPAL-RT simulator. The simulator is connected to the RIAPS nodes (running the IMCP controller code) via Modbus/TCP connections. The code base also includes a Graphical User Interface (GUI) for IMCP that allows an operator to interact with the microgrid controller. The GUI is customized for the Banshee model, it shows the main power values, lets the operator open and close breakers, initiate disconnect and reconnect operations on the feeder connections.

- https://github.com/RIAPS/app.IMCP The main repository of the IMCP code base, with explanations for installing and testing the application.

The repository contains the documentation for setting up and running the entire IMCP application. Two configurations are available: (1) the simpler single-feeder (a.k.a. Vanderbilt) variant, and (2) the more complex 3-feeder (a.k.a.) NCSU variant.

AUXILIARY REPOSITORIES (USED BY IMCP)

Although the IMCP repository is self-contained, it uses several libraries that are not IMCP-specific. These repositories contain the original code of those libraries.

- RIAPS Modbus Interface library https://github.com/RIAPS/interface.modbus.libs This repository contains the source code used to access Modbus devices (via the serial line and TCP protocols) from RIAPS applications.
- RIAPS MQTT Interface library https://github.com/RIAPS/interface.mqtt This repository is for the source used to publish and receive messages to and from an MQTT message broker server.

In the IMCP application the first library is used in to communicate with Modbus devices and the second library is for communicating with the GUI.

LIST OF SCIENTIFIC/TECHNICAL PUBLICATIONS

H. Tu, Y. Du, H. Yu, X. Lu and S. Lukic, "Privacy-Preserving Robust Consensus for Distributed Microgrid Control Applications," in IEEE Transactions on Industrial Electronics, doi: 10.1109/TIE.2023.3274846

H. Tu, Y. Du, H. Yu, S. Meena, X. Lu and S. Lukic, "Distributed Economic Dispatch for Microgrids Tracking Ramp Power Commands," in IEEE Transactions on Smart Grid, vol. 14, no. 1, pp. 94-111, Jan. 2023, doi: 10.1109/TSG.2022.3189534.

P. Ghosh, H. Tu, T. Krentz, G. Karsai and S. Lukic, "An Automated Deployment and Testing Framework for Resilient Distributed Smart Grid Applications," 2022 IEEE International Conference on Omni-layer Intelligent Systems (COINS), Barcelona, Spain, 2022, pp. 1-6, doi: 10.1109/COINS54846.2022.9854934.

S. Meena, H. Tu, H. Yu and S. Lukic, "Economic Dispatch in Microgrids using Relaxed Mixed Integer Linear Programming," 2022 IEEE Energy Conversion Congress and Exposition (ECCE), Detroit, MI, USA, 2022, pp. 1-8, doi: 10.1109/ECCE50734.2022.9947665.

OTHER SUPPORTING MATERIALS

Attached the pre-print of a paper titled “An IoT-based Framework for Distributed Generic Microgrid Controllers” that provides technical details about the microgrid controller.